

Constraints on B and Higgs Physics in Minimal Low Energy Supersymmetric Models

M. Carena^a, A. Menon^{b,c}, R. Noriega-Papaqui^{a,e},
A. Szykman^{a,d,f} and C.E.M. Wagner^{b,c}

^a*Theoretical Physics Dept., Fermi National Laboratory, Batavia, IL 60510*

^b*HEP Division, Argonne National Laboratory, 9700 Cass Ave., Argonne, IL 60439, USA*

^c*Enrico Fermi Inst., Univ. of Chicago, 5640 S. Ellis Ave., Chicago, IL 60637, USA*

^d*Lab. de Phys. Nucleaire, Univ. de Montreal, C.P. 6128, Montreal, Canada H3C 3J7*

^e*Inst. de Física, Univ. Autónoma de Puebla. A. P. J-48 Puebla, México*

^f*IFLP, Dept. de Física, Univ. Nacional de La Plata, C.C. 67, 1900 La Plata Argentina*

August 29, 2018

Abstract

We study the implications of minimal flavor violating low energy supersymmetry scenarios for the search of new physics in the B and Higgs sectors at the Tevatron collider and the LHC. We show that the already stringent Tevatron bound on the decay rate $B_s \rightarrow \mu^+ \mu^-$ sets strong constraints on the possibility of generating large corrections to the mass difference ΔM_s of the B_s eigenstates. We also show that the $B_s \rightarrow \mu^+ \mu^-$ bound together with the constraint on the branching ratio of the rare decay $b \rightarrow s \gamma$ has strong implications for the search of light, non-standard Higgs bosons at hadron colliders. In doing this, we demonstrate that the former expressions derived for the analysis of the double penguin contributions in the Kaon sector need to be corrected by additional terms for a realistic analysis of these effects. We also study a specific non-minimal flavor violating scenario, where there are flavor changing gluino-squark-quark interactions, governed by the CKM matrix elements, and show that the B and Higgs physics constraints are similar to the ones in the minimal flavor violating case. Finally we show that, in scenarios like electroweak baryogenesis which have light stops and charginos, there may be enhanced effects on the B and K mixing parameters, without any significant effect on the rate of $B_s \rightarrow \mu^+ \mu^-$.

1 Introduction

The standard model (SM) provides an accurate description of all the results from high energy physics experiments, in particular precision electroweak measurements and flavor physics observables. These experiments put strong constraints on extensions of the SM that have tree-level flavor changing neutral current effects or large custodial symmetry breaking effects. For renormalizable, weakly interacting theories, where the new exotic particles acquire large gauge invariant masses so that they decouple from the low energy effective theory, these constraints can be avoided. Low energy supersymmetry [1, 2] is a particularly attractive example of this kind of theory. The minimal supersymmetric extension of the Standard Model or MSSM (with gauge invariant SUSY breaking masses of the order of 1 TeV) predicts an extended Higgs sector with a light SM-like Higgs boson of mass lower than 135 GeV [3]–[13] that agrees well with precision electroweak measurements.

However the structure of supersymmetry breaking parameters is not well defined. If there are no tree-level flavor changing transitions in any gauge or super-gauge interaction, then the deviations from SM predictions are naturally small. Such small deviations can be achieved if the quark and squark mass matrices are block diagonalizable in the same basis. For instance, this happens when the squark and slepton supersymmetry breaking masses are flavor independent. For these kinds of models, all flavor violating effects are induced at the loop-level and are governed by the CKM matrix elements, as in the SM. Many studies have concentrated on the properties of these minimal flavor violating scenarios (see, for example, Refs. [14]–[23]).

In this article we shall analyze their flavor violating effects in two quite generic cases. In the first case, we consider a low energy effective theory in which the quark and squark mass matrices are aligned in flavor space and can be simultaneously diagonalized in blocks, as described in the next section. We will remain agnostic about how this effective low energy theory is UV completed. However, since the Yukawa-induced radiative corrections to the soft supersymmetry breaking parameters tend to destroy the alignment of the squark and quark mass matrices, this situation may be only naturally realized in models of low energy supersymmetry breaking, where these radiative corrections are small. We call this low energy scenario Minimal Flavor Violation.

In order to study the possible effect of Yukawa dependent radiative corrections we study a second case, in which we assume a departure from the alignment condition by the presence of flavor violating effects proportional to the CKM matrix elements. These effects are induced by corrections to the left-handed down squark mass matrices proportional to the product of the up-quark Yukawa matrix and its hermitian conjugate (or, in general, powers of this product). We furthermore assume that the right-handed down squark masses are flavor independent. As we will discuss in more detail in the next section, these conditions at low energies are achieved, for instance, by Yukawa dependent radiative corrections, if one starts from flavor independent squark masses at a high energy scale at moderate values of $\tan\beta$. One characteristic of this second scenario is that there are flavor violating down-squark-gluino vertices at tree-level. Since all flavor violating effects are governed by the CKM

matrix elements, this scenario would also enter within the general definition of minimal flavor violating models given in Ref. [21]. However, due to the presence of flavor violating couplings at tree level, we will denote it as non-minimal flavor violation in order to distinguish it from the first scenario of flavor alignment at the weak scale, in which such tree-level effects are absent. As we will show, the phenomenological predictions in this scenario are similar to those of the flavor alignment case, unless the left-handed squarks and the gluino are very light.

Apart from the structure of supersymmetry breaking parameters, the phases associated with them are also important. In minimal flavor violating schemes there are at least two phases that cannot be absorbed by redefining the low energy fields. For real values of the μ parameter, these phases can be associated with a universal phase for the gaugino masses and the trilinear mass parameter. In general, however, one can choose independent phases for the different gaugino masses and trilinear mass parameters. CP-violating phases beyond the CKM one are required, for instance, in models of electroweak baryogenesis [24]–[29]. In this scenario, there could be significant effects on ΔM_s , $\mathcal{BR}(B_s \rightarrow \mu^+\mu^-)$ and ϵ_K because of the presence of a light stop and extra phases in the chargino, neutralino and gluino sectors. We shall comment on the effects of these new CP violating phases below.

In this paper we attempt to develop a systematic method of treating the extra sources of flavor violation in the minimal and non-minimal flavor violating models described above. We show that the usual approach of calculating $\tan\beta$ enhanced FCNC (Flavor Changing Neutral Currents) effects in the Kaon sector does not agree with the exact results one finds in the limit of flavor independent masses. Thus, we develop a perturbative approach that leads to agreement with the exact result in this limit.

We shall emphasize the implications of the present bounds on $\mathcal{BR}(B_s \rightarrow \mu^+\mu^-)$ for future measurements at the Tevatron collider, both in Higgs as well as in B-physics. In particular, we shall show that the present bound on $\mathcal{BR}(B_s \rightarrow \mu^+\mu^-)$ leads to strong constraints on possible corrections to both ΔM_s and the Kaon mixing parameters in minimal flavor violating schemes. Moreover, we shall show that this bound, together with the constraint implied by the measurement of $\mathcal{BR}(b \rightarrow s\gamma)$ leads to limits on the possibility detecting light, non-standard Higgs bosons in the MSSM at the Tevatron collider. Throughout the paper we always take real values of μA_t , and therefore the Higgs sector is approximately CP-invariant [33, 34], and will be treated as such.

This article is organized as follows. In section 2, we define our theoretical setup, giving the basic expressions necessary for the analysis of the flavor violating effects at large values of $\tan\beta$. In particular, we show how the first order perturbative expressions in the CKM matrix elements are inappropriate to define the corrections in the Kaon sector where higher order effects need to be considered. In section 3 we show the implications of the constraint on $\mathcal{BR}(B_s \rightarrow \mu^+\mu^-)$ for the mixing parameters of the Kaon and B sectors in the large $\tan\beta$ regime. In section 4, we explain the implications for Higgs searches at the Tevatron. We reserve section 5 for our conclusions and some technical details for the appendices.

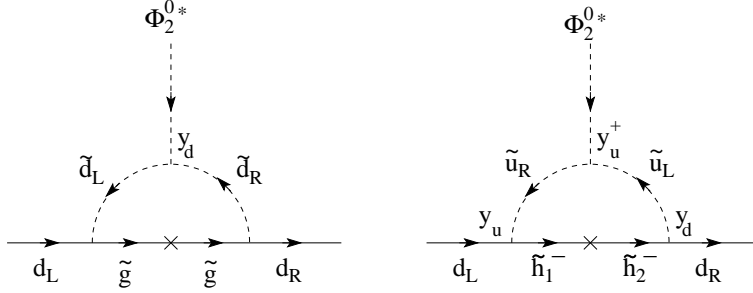


Figure 1: SUSY radiative corrections to the self-energies of the d-quarks in the mass insertion approximation

2 Theoretical Setup

2.1 The resummed effective Lagrangian and the sparticle spectrum

The importance of large $\tan \beta$ FCNC effects in supersymmetry has been known for sometime. The finite pieces of the one-loop self energy diagrams lead to an effective lagrangian for the quark-Higgs sector, valid at energy scales lower than the heavy squark masses, which has the generic form [15]–[20], [30, 31]

$$-\mathcal{L}_{eff} = \bar{d}_R^0 \hat{\mathbf{Y}}_d [\Phi_d^{0*} + \Phi_u^{*0} (\hat{\epsilon}_0 + \hat{\epsilon}_Y \hat{\mathbf{Y}}_u^\dagger \hat{\mathbf{Y}}_u)] d_L^0 + \Phi_u^0 \bar{u}_R^0 \hat{\mathbf{Y}}_u u_L^0 + h.c. \quad (1)$$

$$-\mathcal{L}_{mass} = \frac{v_d}{\sqrt{2}} \bar{d}_R^0 \hat{\mathbf{Y}}_d [1 + \tan \beta (\hat{\epsilon}_0 + \hat{\epsilon}_Y \hat{\mathbf{Y}}_u^\dagger \hat{\mathbf{Y}}_u)] d_L^0 + \frac{v_u}{\sqrt{2}} \bar{u}_R^0 \hat{\mathbf{Y}}_u u_L^0 + h.c. \quad (2)$$

in an arbitrary basis. The $\hat{\epsilon}_0$ and $\hat{\epsilon}_Y$ matrices correspond to radiative contributions [32] coming from the loops shown in Fig. 1. Their exact dependence on the supersymmetric mass parameters is given in Appendix A.2.

The flavor structure of the loop correction factors are independent of their momentum integrations. Therefore, in an arbitrary basis, the flavor dependence of the loop correction parameters are the same as that of the mass matrices and Yukawa couplings. Thus, the loop correction factors have the following flavor structure

$$\hat{\mathbf{Y}}_d \hat{\epsilon}_0 \propto \hat{\mathbf{M}}_{\tilde{d}_R}^{-2} \hat{\mathbf{Y}}_d \hat{\mathbf{M}}_{\tilde{d}_L}^{-2} \quad (3)$$

$$\hat{\mathbf{Y}}_d \hat{\epsilon}_Y \hat{\mathbf{Y}}_u^\dagger \hat{\mathbf{Y}}_u \propto \hat{\mathbf{Y}}_d \hat{\mathbf{M}}_{\tilde{u}_L}^{-2} \hat{\mathbf{Y}}_u^\dagger \hat{\mathbf{M}}_{\tilde{u}_R}^{-2} \hat{\mathbf{Y}}_u \quad (4)$$

where $\hat{\mathbf{M}}^{-2}$ matrices are the non-diagonal inverse squark mass squared matrices. Thus the sparticle spectrum is intimately connected to the ϵ parameters which in turn affect the FCNC's. We look at two possible choices that connect the quark mass eigenstate basis to that of the squarks.

2.1.1 Minimal Flavor Violation

This scenario is similar to that discussed in Refs. [17, 19, 15, 16], where one assumes an alignment of the quark and squark mass matrices in flavor space. Therefore, in the low energy effective theory, the diagonalization of the quark mass matrices leads to squark mass matrices that are block diagonal. Using the following transformation matrices

$$u_L^0 = \mathbf{U}_L^{\mathbf{Q}} u_L, \quad d_L^0 = \mathbf{U}_L^{\mathbf{Q}} \mathbf{V}_0 d_L, \quad u_R^0 = \mathbf{U}_R^{\mathbf{u}} u_R, \quad d_R^0 = \mathbf{U}_R^{\mathbf{d}} d_R \quad (5)$$

to rotate the original quark supermultiplets into a basis where the tree level Yukawa couplings are diagonal, we get

$$\begin{aligned} \mathbf{Y}_d &= \mathbf{U}_R^{\mathbf{d}\dagger} \hat{\mathbf{Y}}_d \mathbf{U}_L^{\mathbf{Q}} \mathbf{V}_0; \\ \mathbf{Y}_u &= \mathbf{U}_R^{\mathbf{u}\dagger} \hat{\mathbf{Y}}_u \mathbf{U}_L^{\mathbf{Q}}; \\ \mathbf{M}_{\tilde{d}_R}^{-2} &= \mathbf{U}_R^{\mathbf{d}\dagger} \hat{\mathbf{M}}_{\tilde{d}_R}^{-2} \mathbf{U}_R^{\mathbf{d}}; & \mathbf{M}_{\tilde{d}_L}^{-2} &= \mathbf{V}_0^\dagger \mathbf{U}_L^{\mathbf{Q}\dagger} \hat{\mathbf{M}}_{\tilde{d}_L}^{-2} \mathbf{U}_L^{\mathbf{Q}} \mathbf{V}_0; \\ \mathbf{M}_{\tilde{u}_R}^{-2} &= \mathbf{U}_R^{\mathbf{u}\dagger} \hat{\mathbf{M}}_{\tilde{u}_R}^{-2} \mathbf{U}_R^{\mathbf{u}}; & \mathbf{M}_{\tilde{u}_L}^{-2} &= \mathbf{U}_L^{\mathbf{Q}\dagger} \hat{\mathbf{M}}_{\tilde{u}_L}^{-2} \mathbf{U}_L^{\mathbf{Q}}; \\ \hat{\epsilon}_0 &\propto \mathbf{U}_L^{\mathbf{Q}} \mathbf{V}_0 \mathbf{M}_{\tilde{d}_R}^{-2} \mathbf{M}_{\tilde{d}_L}^{-2} \mathbf{V}_0^\dagger \mathbf{U}_L^{\mathbf{Q}\dagger}; & \hat{\epsilon}_0 &= \mathbf{U}_L^{\mathbf{Q}} \mathbf{V}_0 \epsilon_0 \mathbf{V}_0^\dagger \mathbf{U}_L^{\mathbf{Q}\dagger}; \\ \hat{\epsilon}_Y &\propto \mathbf{U}_L^{\mathbf{Q}} \mathbf{M}_{\tilde{u}_L}^{-2} \mathbf{M}_{\tilde{u}_R}^{-2} \mathbf{U}_L^{\mathbf{Q}\dagger}; & \hat{\epsilon}_Y &= \mathbf{U}_L^{\mathbf{Q}} \epsilon_Y \mathbf{U}_L^{\mathbf{Q}\dagger}; \end{aligned} \quad (6)$$

where the un-hatted mass and Yukawa matrices are diagonal and \mathbf{V}_0 is the tree level CKM matrix. Under this transformation the effective mass lagrangian becomes

$$-\mathcal{L}_{\text{mass}} = \frac{v_d}{\sqrt{2}} \bar{d}_R \mathbf{Y}_d [1 + \tan \beta (\epsilon_0 + \mathbf{V}_0^\dagger \epsilon_Y |\mathbf{Y}_u|^2 \mathbf{V}_0)] d_L + \frac{v_u}{\sqrt{2}} \bar{u}_R \mathbf{Y}_u u_L + h.c. \quad (7)$$

where the ϵ_0 and ϵ_Y terms, defined in Eq. (6) (see also Appendix A, Eq. (137) and Eq. (138)), are diagonal. Therefore the quark mass matrices receive off-diagonal terms proportional to ϵ_Y at the 1-loop level and so need to be re-diagonalized perturbatively. This procedure has been performed in Refs. [17, 19]. However, the calculation of the (2, 1) and (1, 2) components of the neutral-Higgs-quark-quark coupling are affected by additional corrections not included in Refs. [17, 19]. In Appendix A.1 we calculate the corrected couplings which we present here. Defining the down-quark neutral Higgs interaction Lagrangian to be

$$-\mathcal{L} = \bar{d}_R^J (X_{RL}^S)^{JI} d_L^I \phi_S + h.c., \quad (8)$$

we find that the neutral Higgs flavor changing coupling, with $I \neq J$, takes the form

$$(X_{RL}^S)^{JI} = \frac{\bar{m}_{d_J} y_t^2 \Gamma^{JI} (x_u^S - x_d^S \tan \beta)}{v_d (1 + \epsilon_0^J \tan \beta) (1 + \epsilon_3 \tan \beta)} V_{eff}^{3J*} V_{eff}^{3I} \quad (9)$$

where we have ignored the small effects proportional to the first and second generation Yukawa couplings to find $\epsilon_J = \epsilon_0^J + \delta_{3J} \epsilon_Y y_t^2$, x_u^S and x_d^S are the Higgs scalar components on

the neutral Φ_u^{0*} and Φ_d^{0*} fields (see Appendix A, Eq.(117)) and

$$\Gamma^{3I} = \epsilon_Y \quad (10)$$

$$\Gamma^{J3} = \frac{\epsilon_Y(1 + \epsilon_3^* \tan \beta) - \epsilon_Y^*(\epsilon_3 - \epsilon_J) \tan \beta}{1 + \epsilon_0^{3*} \tan \beta} \quad (11)$$

$$\Gamma^{21} = \frac{\epsilon_Y}{(1 + \epsilon_2 \tan \beta)|1 + \epsilon_0^3 \tan \beta|^2} [(1 + \epsilon_0^3 \tan \beta)|1 + \epsilon_3 \tan \beta|^2 - \epsilon_Y y_t^2 \tan \beta (1 + \epsilon_3^* \tan \beta)(1 + \epsilon_2 \tan \beta) - \epsilon_Y^* y_t^2 \tan \beta (1 + \epsilon_2 \tan \beta)^2] \quad (12)$$

$$\Gamma^{12} = \frac{\epsilon_Y}{(1 + \epsilon_2 \tan \beta)|1 + \epsilon_0^3 \tan \beta|^2} \left\{ (1 + \epsilon_0^3 \tan \beta)|1 + \epsilon_3 \tan \beta|^2 - \epsilon_Y y_t^2 \tan \beta (1 + \epsilon_3^* \tan \beta)(1 + \epsilon_2 \tan \beta) - \epsilon_Y^* y_t^2 \tan \beta (1 + \epsilon_2 \tan \beta)(1 + \epsilon_1 \tan \beta) + \frac{\epsilon_1 - \epsilon_2}{\epsilon_Y} \left[\frac{\epsilon_Y^* \tan \beta}{1 + \epsilon_2^* \tan \beta} - \frac{(\epsilon_Y^*)^2 y_t^2 \tan^2 \beta}{(1 + \epsilon_2^* \tan \beta)(1 + \epsilon_3^* \tan \beta)} - \frac{|\epsilon_Y|^2 y_t^2 \tan^2 \beta}{|1 + \epsilon_3 \tan \beta|^2} \right] \right\}. \quad (13)$$

Here V_{eff} is the CKM matrix obtained after diagonalization of the one-loop mass matrix in Eq. (7). The relation between this matrix and V_0 is given in the Appendix A.1. Observe that in the limit of universal squark soft SUSY breaking masses the ϵ_0 diagonal matrix is proportional to the identity and, in spite of their complicated form, all the Γ^{IJ} become equal to ϵ_Y . The difference between the above expressions and those obtained before in the literature will be discussed in more detail below.

2.1.2 Non-minimal Flavor Violation using the CKM matrix

As explained in the introduction, we shall discuss a second scenario in which all flavor violating effects are proportional to CKM matrix elements, and there are tree-level down-squark-gluino flavor violating vertices in the low energy effective theory. This scenario is similar to that discussed in Ref. [20]. For the present discussion, let us assume that we perform the diagonalization procedure in a single step under the transformation

$$u_L^0 = \mathbf{U}_L^{\mathbf{Q}} u_L, \quad d_L^0 = \mathbf{U}_L^{\mathbf{Q}} \mathbf{V}_{eff} d_L, \quad u_R^0 = \mathbf{U}_R^{\mathbf{u}} u_R, \quad d_R^0 = \mathbf{U}_R^{\mathbf{d}} d_R \quad (14)$$

where instead of \mathbf{V}_0 the tree level CKM matrix we have \mathbf{V}_{eff} the effective CKM matrix. This transformation leads to a diagonal quark mass matrix and a mass lagrangian of the form

$$- \mathcal{L}_{mass} = \frac{v_d}{\sqrt{2}} \bar{d}_R \mathbf{U}_R^{d\dagger} \hat{\mathbf{Y}}_{\mathbf{d}} \mathbf{U}_L^{\mathbf{Q}} [1 + \tan \beta (\epsilon_0 + \epsilon_Y |\mathbf{Y}_{\mathbf{u}}|^2)] \mathbf{V}_{eff} d_L + \frac{v_u}{\sqrt{2}} \bar{u}_R \mathbf{Y}_{\mathbf{u}} u_L + h.c., \quad (15)$$

under the assumption that the matrices

$$\begin{aligned} \epsilon_0 &= \mathbf{U}_L^{\mathbf{Q}\dagger} \hat{\epsilon}_0 \mathbf{U}_L^{\mathbf{Q}} \\ \epsilon_Y &= \mathbf{U}_L^{\mathbf{Q}\dagger} \hat{\epsilon}_Y \mathbf{U}_L^{\mathbf{Q}} \end{aligned} \quad (16)$$

are diagonal [20]. The condition that $\mathbf{U}_L^{\mathbf{Q}\dagger} \hat{\epsilon}_Y \mathbf{U}_L^{\mathbf{Q}}$ is diagonal is the same as Eq. (6) in Minimal Flavor Violation. Thus we again need the u-squark mass matrix to be block diagonal in the u-quark eigenbasis. Therefore there are no flavor changing effects in the neutral up supergauge currents.

However the assumption that $\mathbf{U}_L^{\mathbf{Q}\dagger} \hat{\epsilon}_0 \mathbf{U}_L^{\mathbf{Q}}$ is diagonal differs from Eq. (6) in MFV. From the flavor structure of $\hat{\epsilon}_0$ in Eq.(3), we see that this can only be naturally fulfilled if

$$\mathbf{M}_{\tilde{d}_L}^{-2} = \mathbf{U}_L^{\mathbf{Q}\dagger} \hat{\mathbf{M}}_{\tilde{d}_L}^{-2} \mathbf{U}_L^{\mathbf{Q}}, \quad \text{and} \quad \mathbf{M}_{\tilde{d}_R}^{-2} = \mathbf{U}_R^{\mathbf{d}\dagger} \hat{\mathbf{M}}_{\tilde{d}_R}^{-2} \mathbf{U}_R^{\mathbf{d}} \quad (17)$$

are diagonal and $[\mathbf{M}_{\tilde{d}_R}^{-2}, \mathbf{Y}_d \mathbf{V}_{\text{eff}}^\dagger] = 0$. The obvious way of satisfying this commutation relation is to require the right-handed d-squark mass matrix to be flavor independent or $\mathbf{M}_{\tilde{d}_R}^2 \propto \mathbf{I}$. Observe that this analysis was not performed in Ref. [20] and hence the above conditions were not required in that work. As stressed in the introduction, the above flavor structure of mass matrices may be achieved by Yukawa induced radiative corrections to universal, flavor independent squark masses at high energy scales, at moderate values of $\tan \beta$. Assuming the squark masses are flavor independent at high energies, the only one-loop corrections that violate flavor are induced by the up and down Yukawa matrices because the gauge interactions are flavor blind. These corrections are given by [22]

$$\Delta M_{\tilde{Q}}^2 \simeq -\frac{1}{8\pi^2} \left[(2m_0^2 + M_{H_u}^2(0) + A_0^2) Y_u^\dagger Y_u + (2m_0^2 + M_{H_d}^2(0) + A_0^2) Y_d^\dagger Y_d \right] \log \left(\frac{M}{M_{SUSY}} \right), \quad (18)$$

where \tilde{Q} denote the left-handed squarks, m_0 is the common squark mass at the scale M at which supersymmetry breaking is transmitted to the observable sector, $M_{H_{u,d}}^2(0)$ and A_0 are the Higgs soft supersymmetry breaking masses and squark-Higgs trilinear mass parameters at that scale, and M_{SUSY} is the characteristic low energy squark mass scale.

Similarly, the right-handed up and down squark mass matrices, receive one-loop Yukawa-induced corrections proportional to

$$\Delta M_{\tilde{u}_R}^2 = -\frac{2}{8\pi^2} (2m_0^2 + M_{H_u}^2(0) + A_0^2) Y_u Y_u^\dagger \log \left(\frac{M}{M_{SUSY}} \right), \quad (19)$$

and

$$\Delta M_{\tilde{d}_R}^2 = -\frac{2}{8\pi^2} (2m_0^2 + M_{H_d}^2(0) + A_0^2) Y_d Y_d^\dagger \log \left(\frac{M}{M_{SUSY}} \right), \quad (20)$$

respectively.

Therefore, while the Yukawa induced radiative corrections to the right-handed squark mass matrices maintain the alignment of these matrices with their corresponding Yukawa matrices, the corrections to the left-handed squark masses induced a misalignment between the quark and squark mass matrices governed by CKM matrix elements. Since the dominant effects are governed by the third generation Yukawa eigenvalues, the down-quark Yukawa effects may be neglected at small or moderate values of $\tan \beta$ where the bottom Yukawa coupling is much smaller than the top quark one. In this case, one arrives at the properties

of the squark mass matrices specified in the non-minimal flavor violating scenario defined above.

In general, even at larger values of $\tan\beta$, the only flavor violating squark-gluino vertices will be in the left-handed couplings (and the Higgs-squark-squark vertices) and they will be governed by CKM matrix elements. The only difference between the large $\tan\beta$ case with respect to the non-minimal flavor violating model defined above is that the masses of the right-handed down squarks will no longer be flavor independent at low energies and therefore the $\hat{\epsilon}_0$ matrix will not be aligned with the $\hat{\epsilon}_Y$ one. However, the flavor properties of the large $\tan\beta$ scenario are quite similar the non-minimal flavor violating scenario specified above and therefore this scenario will allow us to study the possible effects of the Yukawa induced radiative corrections to the squark mass matrices, in particular the ones associated with the flavor violating down-squark-gluino couplings at tree-level.

Following the argument in Ref. [20] we can rewrite the effective lagrangian in terms of the mass eigenstates as

$$\begin{aligned}
-\mathcal{L}_{eff} = & \frac{\sqrt{2}}{v_u}(\Phi_d^{0*} - \Phi_u^{0*} \tan\beta)\bar{d}_R\bar{\mathbf{m}}_d V_{eff}^\dagger \mathbf{R}^{-1} V_{eff} d_L + \frac{\sqrt{2}}{v_u}\Phi_u^{0*}\bar{d}_R\bar{\mathbf{m}}_d d_L \\
& + \Phi_u^0 \bar{u}_R \mathbf{Y}_u u_L + h.c.
\end{aligned} \tag{21}$$

where V_{eff} is the effective CKM matrix, \mathbf{Y}_u is the diagonal up Yukawa matrix, $\bar{\mathbf{m}}_d$ is the diagonal down-quark running mass matrix, and

$$\mathbf{R} = \mathbf{1} + \epsilon_0 \tan\beta + \epsilon_Y |\mathbf{Y}_u|^2 \tan\beta. \tag{22}$$

Therefore, neglecting¹ y_u and y_c as compared to y_t , and defining

$$\epsilon_J = \epsilon_0^J + \epsilon_Y y_t^2 \delta^{J3} \tag{23}$$

for all J , we find

$$(\mathbf{R}^{-1})^{JI} = \frac{1}{1 + \epsilon_J \tan\beta} \delta^{JI} \tag{24}$$

If we assume a generational mass splitting so that the first two generations are equally massive and heavier than the third generation we find $\epsilon_0^1 = \epsilon_0^2 = \epsilon_0$. In this case the flavor changing effects are not solely dependent on ϵ_Y , but they also depend on the difference between the loop factors ($\epsilon_3 - \epsilon_0$):

$$(X_{RL}^S)^{JI} = \frac{\bar{m}_{d_J}(\epsilon_3 - \epsilon_0)(x_u^S - x_d^S \tan\beta)}{v_d(1 + \epsilon_0 \tan\beta)(1 + \epsilon_3 \tan\beta)} V_{eff}^{3J*} V_{eff}^{3I}. \tag{25}$$

The reason we call this scenario non-minimal flavor violation is that the diagonalization procedure induces flavor changing effects in the gluino-quark-squark couplings which lead to

¹This approximation breaks down in the limit $1 + \epsilon_0 \tan\beta \rightarrow 0$, the singularity in $[X_{RL}^{dS}]$ proportional to y_t cancels against those coming from y_c and y_u as discussed in Ref. [20]

additional contributions to flavor changing processes. Indeed, the assumption that ϵ_0 and ϵ_Y in Eq.(16) are diagonal leads to the appearance of CKM elements in the down quark-squark-gluino coupling, as it is clear from Eqs. (14) and (17). Because the left-handed squarks are not diagonalized by the same rotation as the left-handed quarks, the effective gluino Lagrangian becomes

$$\begin{aligned} \mathcal{L}_{\tilde{g}} = & -\sqrt{2}g_s [\bar{u}_L \tilde{g}^a T^a \tilde{u}_L - \bar{u}_R \tilde{g}^a T^a \tilde{u}_R] \\ & +\sqrt{2}g_s [\bar{d}_L \tilde{g}^a T^a \mathbf{V} \tilde{d}_L - \bar{d}_R \tilde{g}^a T^a \tilde{d}_R]. \end{aligned} \quad (26)$$

The appearance of the CKM matrix in the gluino couplings induces flavor changing box diagrams that can in principle produce large effects.

2.1.3 The uniform squark mass limit

The two flavor changing scenarios discussed above coincide for the case of uniform squark masses. Since, in this limit, the transformation performed in Section 2.1.2 requires no approximations or assumptions the expression for the FCNC's are exact. However, the perturbative approach in Section 2.1.1 provides expressions for the FCNCs that are only valid up to a certain order in the off-diagonal CKM matrix elements. For the perturbative approach in Section 2.1.1 to be valid we need the two expression for the FCNC's to be equal to at least quadratic order in the off-diagonal CKM matrix elements. However, as discussed above, comparing the results of Ref. [19] and Ref. [20] this is clearly not true for the (2, 1) and (1, 2) components of the down quark-Higgs couplings X_{RL} .

In the uniform squark limit, the flavor violating coupling given in Eq. (25) has the form

$$(X_{RL}^S)^{JI} = \frac{\bar{m}_{d_J} \epsilon_Y y_t^2 (x_u^S - x_d^S \tan \beta)}{v_d (1 + \epsilon_3 \tan \beta) (1 + \epsilon_0 \tan \beta)} V_{eff}^{3J*} V_{eff}^{3I}. \quad (27)$$

which does not agree with the results in Ref. [19], where they find the corrected coupling to be

$$(X_{RL}^S)^{21} = \frac{\bar{m}_{d_J} \epsilon_Y y_t^2}{v_d} \frac{|1 + \epsilon_3 \tan \beta|^2}{|1 + \epsilon_0 \tan \beta|^2 (1 + \epsilon_0 \tan \beta)^2} V_{eff}^{3J*} V_{eff}^{3I5} (x_u^S - x_d^S \tan \beta). \quad (28)$$

To understand this difference between the results of Ref. [19] and Ref. [20] we need to look at the approximations made in Ref. [19]. Diagonalizing the tree level quark mass matrices in Eq. (7) leads to uncorrected diagonal masses \mathbf{m}_d and a CKM matrix \mathbf{V}_0 . However the large $\tan \beta$ enhanced radiative corrections lead to off-diagonal terms in the mass matrix, which have the form

$$(\mathbf{m}_d + \Delta \mathbf{m}_d)^{JI} = m_{d_J} ((1 + \epsilon_J \tan \beta) \delta^{JI} + \epsilon_Y y_t^2 \tan \beta \lambda_0^{JI}) \quad (29)$$

where $\lambda_0^{JI} = V_0^{3J*} V_0^{3I}$ for $J \neq I$ and ϵ_J is defined in eqn. (23). We have also neglected contributions to the diagonal elements of the form $|V_0^{3J}|^2$ for $J \neq 3$ as they are subdominant.

Hence, to go to the physical quark basis we need to further diagonalize this effective mass matrix by unitary matrices $\mathbf{D}_{\mathbf{L},\mathbf{R}}$ so that

$$e^{-i\theta_J}(\mathbf{D}_{\mathbf{R}}^\dagger(\mathbf{m}_d + \Delta\mathbf{m}_d)\mathbf{D}_{\mathbf{L}})^{JI} = \bar{m}_{d_J}\delta^{JI} \quad (30)$$

where $\theta_J = \arg(1 + \epsilon_J \tan \beta)$. The approach taken in Ref. [19] is to perturbatively expand the diagonalization matrices $\mathbf{D}_{\mathbf{L}}$ and $\mathbf{D}_{\mathbf{R}}$ so that

$$\mathbf{D}_{\mathbf{L}} = \mathbf{1} + \Delta\mathbf{D}_{\mathbf{L}} \quad (31)$$

$$\mathbf{D}_{\mathbf{R}} = \mathbf{1} + \Delta\mathbf{D}_{\mathbf{R}} \quad (32)$$

where the unitarity of $\mathbf{D}_{\mathbf{L},\mathbf{R}}$ to linear order in Δ leads to conditions $(\Delta\mathbf{D}_{\mathbf{L},\mathbf{R}})^\dagger = -\Delta\mathbf{D}_{\mathbf{L},\mathbf{R}}$, so that when $J \neq I$ in Eq.(30) we have the condition

$$e^{-i\theta_J}(-(\Delta\mathbf{D}_{\mathbf{R}})\bar{\mathbf{m}}_d + \Delta\mathbf{m}_d + \bar{\mathbf{m}}_d(\Delta\mathbf{D}_{\mathbf{L}}))^{JI} = 0, \quad (33)$$

where the \bar{m}_d includes higher order terms and higher orders in Δ have been neglected. Using Eq. (33) and its dagger along with the hierarchy in quark masses gives us

$$(\Delta\mathbf{D}_{\mathbf{L}})^{JI} = \begin{cases} -\frac{\epsilon_Y y_t^2 \tan \beta}{1 + \epsilon_J \tan \beta} \lambda_0^{JI} & J > I \\ \frac{\epsilon_Y^* y_t^2 \tan \beta}{1 + \epsilon_J^* \tan \beta} \lambda_0^{JI} & J < I \end{cases} \quad (34)$$

and

$$(\Delta\mathbf{D}_{\mathbf{R}})^{JI} = \begin{cases} -\frac{\bar{m}_{d_I}}{\bar{m}_{d_J}} \left(\frac{\epsilon_Y y_t^2 \tan \beta}{1 + \epsilon_J \tan \beta} + \frac{\epsilon_Y^* y_t^2 \tan \beta}{1 + \epsilon_J^* \tan \beta} \right) e^{i(\theta_J - \theta_I)} \lambda_0^{JI} & J > I \\ \frac{\bar{m}_{d_J}}{\bar{m}_{d_I}} \left(\frac{\epsilon_Y y_t^2 \tan \beta}{1 + \epsilon_I \tan \beta} + \frac{\epsilon_Y^* y_t^2 \tan \beta}{1 + \epsilon_I^* \tan \beta} \right) e^{i(\theta_J - \theta_I)} \lambda_0^{JI} & J < I \end{cases} \quad (35)$$

Putting these matrices back into Eq. (33) with $(J, I) = (2, 1)$ the dominant terms have the form

$$e^{-i\theta_2}(\bar{\mathbf{m}}_d \Delta\mathbf{D}_{\mathbf{L}})^{21} = -\frac{\bar{m}_s \epsilon_Y y_t^2 \tan \beta}{1 + \epsilon_2 \tan \beta} \lambda_0^{21}, \quad (36)$$

which are comparable to the terms that were neglected in Eq. (33) like

$$e^{-i\theta_2}((\Delta\mathbf{m}_d)(\Delta\mathbf{D}_{\mathbf{L}}))^{21} = -\frac{\bar{m}_s \epsilon_Y^2 y_t^4 \tan^2 \beta}{(1 + \epsilon_2 \tan \beta)(1 + \epsilon_3 \tan \beta)} \lambda_0^{21}. \quad (37)$$

This is particularly true for values of $\epsilon_3 < 0$ and large values of $\tan \beta$. Therefore the deviation between Ref. [20] and Ref. [19] in the Kaon sector is due to a breakdown in the perturbative series leading to first and second order contributions being comparable. The expansion shown in Ref. [19] works for the (1, 3), (2, 3), (3, 1) and (3, 2) components as they expanded the mass matrices only to first order. As mentioned above, an analysis of the second order corrections, together with a derivation of Eqs. (12)–(13) is presented in Appendix A.1.

2.1.4 Flavor changing in the Charged Higgs Coupling

The process of calculating the flavor changing couplings for the charged goldstone modes is exactly the same as in Ref. [19]. As the couplings of the goldstone has to match those of the W-bosons at tree level, so as to form its longitudinal mode, the flavor changing effects have to be

$$(P_{LR}^{G+})^{JI} = -\frac{\sqrt{2}}{v} V_{eff}^{JI} \bar{m}_{dI} \quad (38)$$

$$(P_{RL}^{G+})^{JI} = \frac{\sqrt{2}}{v} \bar{m}_{uI} V_{eff}^{JI} \quad (39)$$

The charged Higgs has the effective lagrangian [31]

$$\begin{aligned} \mathcal{L}_{eff}^{H+} = & \frac{\sqrt{2}}{v} \bar{u}_R \left[\cot \beta \mathbf{m}_u - \frac{v_d}{\sqrt{2}} \tan \beta \Delta \mathbf{Y}_u \right] V_{eff} d_L H^+ + \\ & \frac{\sqrt{2}}{v} \bar{u}_L V_{eff} \mathbf{D}_L^\dagger \left[\tan \beta \mathbf{m}_d - \frac{v_u}{\sqrt{2}} \cot \beta \Delta \mathbf{Y}_d \right] \mathbf{D}_R d_R H^+ \end{aligned} \quad (40)$$

where

$$(\Delta \mathbf{Y}_u)^{JI} = y_{u,J} (\epsilon_0'^J \delta^{JI} + \epsilon_Y' y_b^2 V_0^{J3} V_0^{I3*}) \quad (41)$$

$$(\Delta \mathbf{Y}_d)^{JI} = -y_{d,J} (\epsilon_0^J \delta^{JI} + \epsilon_Y y_t^2 V_0^{3J*} V_0^{3I}) \quad (42)$$

are the generic form of corrections to the down(up) Yukawas after neglecting the Yukawas of the first two generations. The matrices ϵ_0' and ϵ_Y' are closely related to ϵ_0 and ϵ_Y and their form is given in Appendix A.1. Hence, we find for $I = 1, 2, 3$

$$\begin{aligned} (P_{RL}^{H+})^{3I} = & \frac{\sqrt{2}}{v} m_t \cot \beta V_{eff}^{3I} \left(1 - \tan \beta \left(\epsilon_0'^3 \right. \right. \\ & \left. \left. + \epsilon_Y' y_b^2 \left[\frac{1 + \epsilon_3 \tan \beta}{1 + \epsilon_3^0 \tan \beta} \delta^{3I} - \frac{\epsilon_Y y_t^2 \tan \beta}{1 + \epsilon_3^0 \tan \beta} \right] \right) \right), \end{aligned} \quad (43)$$

for $J \neq 3$

$$(P_{RL}^{H+})^{J3} = \frac{\sqrt{2}}{v} m_{u,J} \cot \beta V_{eff}^{J3} \left(1 - \tan \beta \left(\epsilon_0'^J + \epsilon_Y' y_b^2 \frac{1 + \epsilon_3^* \tan \beta}{1 + \epsilon_3^{0*} \tan \beta} \right) \right) \quad (44)$$

and finally for $(J, I) = (2, 1), (1, 2), (1, 1)$ and $(2, 2)$

$$(P_{RL}^{H+})^{JI} = \frac{\sqrt{2}}{v} m_{u,J} \cot \beta V_{eff}^{JI} \left(1 - \tan \beta \epsilon_0'^J \right) \quad (45)$$

which agrees with Ref. [19] if the phases are neglected. To find the left-right coupling we neglect the $(\Delta \mathbf{Y}_d)$ as it is suppressed by $\cot \beta$ so that we have for $I \neq 3$

$$(P_{LR}^{H+})^{3I} = \frac{\sqrt{2}}{v} \frac{\bar{m}_{dI} \tan \beta (1 + \epsilon_3 \tan \beta)}{(1 + \epsilon_0^3 \tan \beta)(1 + \epsilon_3^* \tan \beta)} V_{eff}^{3I} \left(\frac{1 + \epsilon_0^{3*} \tan \beta}{1 + \epsilon_I^* \tan \beta} - \frac{\epsilon_Y y_t^2 \tan \beta}{1 + \epsilon_3 \tan \beta} \right), \quad (46)$$

for $J \neq 3$

$$(P_{LR}^{H+})^{J3} = \frac{\sqrt{2}}{v} \frac{\bar{m}_b \tan \beta}{1 + \epsilon_0^{3*} \tan \beta} V_{eff}^{J3} \quad (47)$$

and for $(J, I) = (3, 3)$ and $J \neq 3 \neq I$

$$(P_{LR}^{H+})^{33} = \frac{\sqrt{2}}{v} \frac{\bar{m}_b \tan \beta}{1 + \epsilon_3^* \tan \beta} V_{eff}^{33} \quad (48)$$

$$(P_{LR}^{H+})^{JI} = \frac{\sqrt{2}}{v} \frac{\bar{m}_{d_I} \tan \beta}{1 + \epsilon_I^* \tan \beta} V_{eff}^{JI} \quad (49)$$

3 Flavor changing processes in the Kaon and B_s -Meson systems

3.1 $\Delta F = 2$ processes

The effective Hamiltonian that contributes to $\Delta F = 2$ processes in the Kaon and B_s meson systems have the generic form

$$\mathcal{H}_{eff}^{\Delta F=2} = \frac{G_f^2 M_W^2}{16\pi^2} \sum_i C_i(\mu) Q_i(\mu) \quad (50)$$

where $C_i(\mu)$ are the Wilson coefficients evaluated at the scale μ . The ΔF operators for a meson of the form $(\bar{q}^J q^I)$ are

$$\begin{aligned} Q^{VLL} &= (\bar{q}_L^J \gamma_\mu q_L^I) (\bar{q}_L^J \gamma^\mu q_L^I) \\ Q_1^{SLL} &= (\bar{q}_R^J q_L^I) (\bar{q}_R^J q_L^I) \\ Q_2^{SLL} &= (\bar{q}_R^J \sigma_{\mu\nu} q_L^I) (\bar{q}_R^J \sigma^{\mu\nu} q_L^I) \\ Q^{VRR} &= (\bar{q}_R^J \gamma_\mu q_R^I) (\bar{q}_R^J \gamma^\mu q_R^I) \\ Q_1^{SRR} &= (\bar{q}_L^J q_R^I) (\bar{q}_L^J q_R^I) \\ Q_2^{SRR} &= (\bar{q}_L^J \sigma_{\mu\nu} q_R^I) (\bar{q}_L^J \sigma^{\mu\nu} q_R^I) \\ Q_1^{LR} &= (\bar{q}_L^J \gamma_\mu q_L^I) (\bar{q}_R^J \gamma^\mu q_R^I) \\ Q_2^{LR} &= (\bar{q}_R^J q_L^I) (\bar{q}_L^J q_R^I) \end{aligned} \quad (51)$$

So for the $K^0 - \bar{K}^0$ system the quantities of interest to us are ϵ_K and the eigenstate mass difference ΔM_K , which to a good approximation have the form

$$\Delta M_K = 2\text{Re}(\langle \bar{K}^0 | H_{eff}^{\Delta S=2} | K^0 \rangle) \quad \epsilon_K = \frac{e^{i\pi/4}}{\sqrt{2}\Delta M_K} \text{Im}(\langle \bar{K}^0 | H_{eff}^{\Delta S=2} | K^0 \rangle). \quad (52)$$

The SUSY contribution to the matrix element for the meson M may be written down as

$$\begin{aligned}
\langle \bar{M} | H_{eff}^{\Delta S=2} | M \rangle^{SUSY} &= \frac{G_f^2 M_W^2}{12\pi^2} m_M F_M^2 \eta_2 \hat{B}_M \left[\bar{P}^{VLL} (C^{VLL}(\mu_{SUSY}) + C^{VRR}(\mu_{SUSY})) + \right. \\
&\quad \bar{P}_1^{SLL} (C_1^{SLL}(\mu_{SUSY}) + C_1^{SRR}(\mu_{SUSY})) + \\
&\quad \bar{P}_2^{SLL} (C_2^{SLL}(\mu_{SUSY}) + C_2^{SRR}(\mu_{SUSY})) \\
&\quad \left. + \bar{P}_1^{LR} C_1^{LR}(\mu_{SUSY}) + \bar{P}_2^{LR} C_2^{LR}(\mu_{SUSY}) \right]. \tag{53}
\end{aligned}$$

For the Kaon system $m_K = 0.498$ GeV, $F_K = 0.16$ GeV, the values of the NLO QCD factors from Ref. [20] are

$$\bar{P}_1^{VLL} = 0.25, \bar{P}_1^{LR} = -18.6, \bar{P}_2^{LR} = 30.6, \bar{P}_1^{SLL} = -9.3, \bar{P}_2^{SLL} = -16.6 \tag{54}$$

for which the values $\eta_2 = 0.57$, $\hat{B}_K = 0.85$ have been used. The dominant contributions as shown in Ref. [19, 20] come from the double penguin diagrams which on matching give contributions to the Wilson coefficients

$$\begin{aligned}
C_2^{LR} &= -\frac{16\pi^2}{G_f^2 (V_{eff}^{21})^2 M_W^2} \sum_{S=1}^3 \frac{1}{M_S^2} (X_{RL}^S)^{21} (X_{LR}^S)^{21} \\
C_1^{SLL} &= -\frac{8\pi^2}{G_f^2 (V_{eff}^{21})^2 M_W^2} \sum_{S=1}^3 \frac{1}{M_S^2} (X_{RL}^S)^{21} (X_{RL}^S)^{21} \\
C_1^{SRR} &= -\frac{8\pi^2}{G_f^2 (V_{eff}^{21})^2 M_W^2} \sum_{S=1}^3 \frac{1}{M_S^2} (X_{LR}^S)^{21} (X_{LR}^S)^{21}. \tag{55}
\end{aligned}$$

Additional subleading contributions at large $\tan\beta$ come from the charged-Higgs boson and chargino box-diagram contributions to ϵ_K , and their form are given in the Appendix A.4 of Ref. [19].

Similarly, for the B_s eigenstate mass differences ΔM_s , using again Eq. (50) for $\Delta B = 2$ processes, we get, approximately,

$$\Delta M_s = 2 |\langle \bar{B}_s | H_{eff}^{\Delta B=2} | B_s \rangle| \tag{56}$$

Therefore, using Eq. (53), the mass difference in the $\bar{B}_s - B_s$ meson system can be found using $m_{B_s} = 5.37$ GeV, $F_{B_s} = 0.230$ GeV and the values of NLO QCD factors from Ref. [19] being

$$\bar{P}_1^{VLL} = 0.254, \bar{P}_1^{LR} = -0.71, \bar{P}_2^{LR} = 0.90, \bar{P}_1^{SLL} = -0.37, \bar{P}_2^{SLL} = -0.72 \tag{57}$$

for which the values $\eta_B = 0.55$, $\hat{B}_{B_s} = 1.3$ have been used. Again, the dominant contributions come from double-penguin diagrams which have the same form as Eq. (55) with the indices $(2, 1) \rightarrow (3, 2)$ and there are subdominant contributions from the box diagrams with charged Higgs bosons and stop-charginos.

3.2 $\Delta F = 1$ processes contributing to $B_s \rightarrow \mu^+ \mu^-$

The effective Hamiltonian that contributes to $\Delta F = 1$ processes in the B_s meson system has the form

$$\mathcal{H}_{eff}^{\Delta B=1} = \frac{G_f \alpha_{em}}{\sqrt{2} \pi s_w^2} V_{eff}^{tb} V_{eff}^{ts} \sum_i c_i(\mu) \mathcal{O}_i(\mu) \quad (58)$$

where the operators \mathcal{O} are

$$\begin{aligned} \mathcal{O}_A &= (\bar{b}_L \gamma^\mu s_L) (\bar{l} \gamma_\mu \gamma_5 l) \\ \mathcal{O}'_A &= (\bar{b}_R \gamma^\mu s_R) (\bar{l} \gamma_\mu \gamma_5 l) \\ \mathcal{O}_S &= m_b (\bar{b}_R s_L) (\bar{l} l) \\ \mathcal{O}'_S &= m_s (\bar{b}_L s_R) (\bar{l} l) \\ \mathcal{O}_P &= m_b (\bar{b}_R s_L) (\bar{l} \gamma_5 l) \\ \mathcal{O}'_S &= m_s (\bar{b}_L s_R) (\bar{l} \gamma_5 l). \end{aligned} \quad (59)$$

The operators \mathcal{O}_A and \mathcal{O}'_A can be dropped as c_A and c'_A are proportional to the muon mass and so are small at large $\tan \beta$. Also the other primed operators are suppressed with respect to the unprimed ones due to the hierarchy of quark masses. So the dominant contributions at large $\tan \beta$ come from the penguin diagrams leading to the contributions

$$\begin{aligned} c_S &= -\frac{4\pi^2 m_\mu \tan \beta}{\bar{m}_b M_W^2 2^{7/4} G^{3/2} V_{eff}^{ts} \sin \beta} \sum_{I=1}^3 \frac{1}{M_I^2} (X_{RL}^I)^{32} O^{1I} \\ c_P &= i \frac{4\pi^2 m_\mu \tan \beta}{\bar{m}_b M_W^2 2^{7/4} G^{3/2} V_{eff}^{ts}} \sum_{I=1}^3 \frac{1}{M_I^2} (X_{RL}^I)^{32} O^{3I}. \end{aligned} \quad (60)$$

where O^{IJ} is the neutral Higgs diagonalization matrix and related to x_u^S and x_d^S through Eq.(117). Hence, in the large $\tan \beta$ limit we find [19]

$$\mathcal{BR}(B_s \rightarrow \mu^+ \mu^-) = 2.32 \times 10^{-6} M_{B_s}^2 (|c_S|^2 + |c_P|^2) \quad (61)$$

4 Numerical Results: Minimal Flavor Violation

In this section we will study some of the phenomenological implications of the scenarios of minimal flavor violation. The quantities of interest in the following section are ΔM_K , ϵ_K , and in particular the observables in the B sector, ΔM_s and $\mathcal{BR}(B_s \rightarrow \mu^+ \mu^-)$. The standard model theoretical prediction of ΔM_s has errors associated with the quantities \bar{m}_t , V_{ts} , and $F_{B_s} \sqrt{B_{B_s}}$ that lead to large theoretical uncertainties [36, 37]. There is good agreement between the central values for the SM prediction for ΔM_s obtained by the CKMfitter and UTFit groups. Their evaluation of the uncertainties is somewhat different. The UTFit group finds the 2σ range [38]

$$16.7 \text{ ps}^{-1} \leq (\Delta M_s)^{SM} \leq 26.9 \text{ ps}^{-1} \quad (62)$$

with central value 21.5 ps^{-1} , which is consistent with the CKMfitter groups' 2σ range [39]

$$14.9 \text{ ps}^{-1} \leq (\Delta M_s)^{SM} \leq 31.4 \text{ ps}^{-1} \quad (63)$$

and central value 21.7 ps^{-1} . Additionally, the D0 collaboration has reported a signal consistent with values of ΔM_s in the range

$$21 (\text{ps})^{-1} > \Delta M_s > 19 \text{ ps}^{-1} \quad (64)$$

at the 90 % confidence level [40]. More recently, the CDF collaboration has made a measurement of ΔM_s [41],

$$\Delta M_s = (17.33_{-0.21}^{+0.42} \pm 0.07(\text{syst}))\text{ps}^{-1}. \quad (65)$$

The experimental bound [42, 43]

$$\mathcal{BR}(B_s \rightarrow \mu^+ \mu^-) \leq 1 \times 10^{-7} \quad (66)$$

puts strong restrictions on possible flavor violating effects induced by the double penguin contributions in the large $\tan \beta$ regime. The dominant contributions for large $\tan \beta$ to ΔM_s and $\mathcal{BR}(B_s \rightarrow \mu^+ \mu^-)$ come from the same penguin diagrams. The dominant contributions to ϵ_0^J and ϵ_Y come from the gluino d-squark loop and the chargino u-squark loop, respectively. Hence, for heavy squarks, the form of these loop corrections can be written approximately as

$$|\epsilon_0^3| \approx \frac{2\alpha_s}{3\pi} |M_3| |\mu| C_0(m_{b_1}^2, m_{b_2}^2, |M_3|^2) \quad (67)$$

$$|\epsilon_Y| \approx \frac{1}{16\pi^2} |A_t| |\mu| C_0(m_{t_1}^2, m_{t_2}^2, |\mu|^2), \quad (68)$$

where C_0 is the standard Passarino-Veltman function.

4.1 Phenomenological constraints on Double Penguin Contributions in the MFV scenario

4.1.1 The effect of $\mathcal{BR}(B_s \rightarrow \mu^+ \mu^-)$ constraint on ΔM_s

As has been shown in Ref. [19] the chargino box diagrams can be neglected if all the squark masses are greater than about 0.5 TeV. We are now interested in setting an upper bound on the FCNC effects induced by the double penguin contributions. From the form of Eq. (67) and Eq. (68) it is clear that the loop integrals are larger for smaller values of the squark masses. The value of ϵ_0 is maximized for large values of μ and for values of M_3 about twice the overall squark mass value. The value of ϵ_Y on the other hand, is maximized for large values of A_t and values of μ that are of order two times the overall squark mass value. At the same time, large values of μ and/or A_t may induce the presence of color breaking

minima [44, 45]. Hence, values of $M_3 \sim 2m_{\tilde{q}} \sim \mu$ maximize ϵ_Y , while pushing ϵ_0 to large values. For these values of the parameters, the loop corrections are given by

$$|(\epsilon_0^3)_{MAX}| \sim 2.7 \times 10^{-2} \quad (69)$$

$$|(\epsilon_Y)_{MAX}| \sim 1 \times 10^{-2}, \quad (70)$$

where we have constrained the trilinear mass parameter $A_t \lesssim 3m_{\tilde{q}}$, so as not to create color breaking minima [44, 45]. Let us stress that the bounds on the parameters coming from color breaking minima may be avoided by assuming metastability of the electroweak symmetry breaking vacuum. However, the somewhat extreme values of the parameters given above induce additional anomalies in the low energy spectrum. For instance, values of $A_t \gtrsim 3.2m_{\tilde{q}}$, decrease the physical Higgs mass to values lower than the current experimental bound on this quantity [3]–[13]. It is also important to stress that for negative values of μM_3 , the coupling X_{RL}^J may be enhanced by taking even larger values of $|\mu|$. Indeed, ϵ_Y only falls off slowly for larger $|\mu|$, while ϵ_0^J increases linearly and therefore X_{RL}^J grows with increasing μ . We shall comment on the effect of taking larger values of $|\mu|$ below.

In the region of large $\tan \beta$ the heavy CP-even and CP-odd masses are approximately equal and the Higgs mixing angle $\alpha \sim 1/\tan \beta$, so that the dominant contribution to $\mathcal{BR}(B_s \rightarrow \mu^+ \mu^-)$ is given by

$$\mathcal{BR}(B_s \rightarrow \mu^+ \mu^-) = 4.64 \times 10^{-6} M_{B_s}^2 \left(\frac{4\pi^2 m_\mu \tan \beta}{\bar{m}_b M_W^2 2^{7/4} G^{3/2} |V_{eff}^{ts}|} \right)^2 \frac{|(X_{RL}^A)^{32}|^2}{M_A^4}. \quad (71)$$

Similarly we find the dominant SUSY contribution to ΔM_s comes from the C_2^{LR} coefficient. To understand why the C_2^{LR} term is dominant over the C_1^{SLL} we consider the case when there is no CP violation in the neutral Higgs sector. In the basis (H^0, h^0, A) we have $x_u^S = (\sin \alpha, \cos \alpha, -i \cos \beta)$ and $x_d^S = (\cos \alpha, -\sin \alpha, i \sin \beta)$, where α is the Higgs mixing angle. Putting these values into Eq.(55) for the $(3, 2)$ component, we find [19],

$$C_2^{LR} \propto \bar{m}_b \bar{m}_s \tan^4 \beta \left(\frac{\sin^2(\alpha - \beta)}{M_{H^0}^2} + \frac{\cos^2(\alpha - \beta)}{M_{h^0}^2} + \frac{1}{M_A^2} \right) \quad (72)$$

$$C_1^{SLL} \propto \bar{m}_b^2 \tan^4 \beta \left(\frac{\sin^2(\alpha - \beta)}{M_{H^0}^2} + \frac{\cos^2(\alpha - \beta)}{M_{h^0}^2} - \frac{1}{M_A^2} \right). \quad (73)$$

From a cursory inspection of these two equation it is not clear which term is dominant, at large $\tan \beta$, as C_2^{LR} is suppressed by a factor of \bar{m}_s/\bar{m}_b with respect to C_1^{SLL} . However, using the constraint equations that relate M_{h^0} , α and β at tree-level in the MSSM [11] we find

$$M_{h^0}^2 \approx M_Z^2 \left(1 - \frac{4}{\tan^2 \beta} \right) \quad (74)$$

$$\frac{\cos^2(\alpha - \beta)}{M_{h^0}^2} = \frac{M_Z^2 - M_{h^0}^2}{M_A^2 (M_{H^0}^2 - M_{h^0}^2)} \approx \frac{4M_Z^2}{M_A^4 \tan^2 \beta} \quad (75)$$

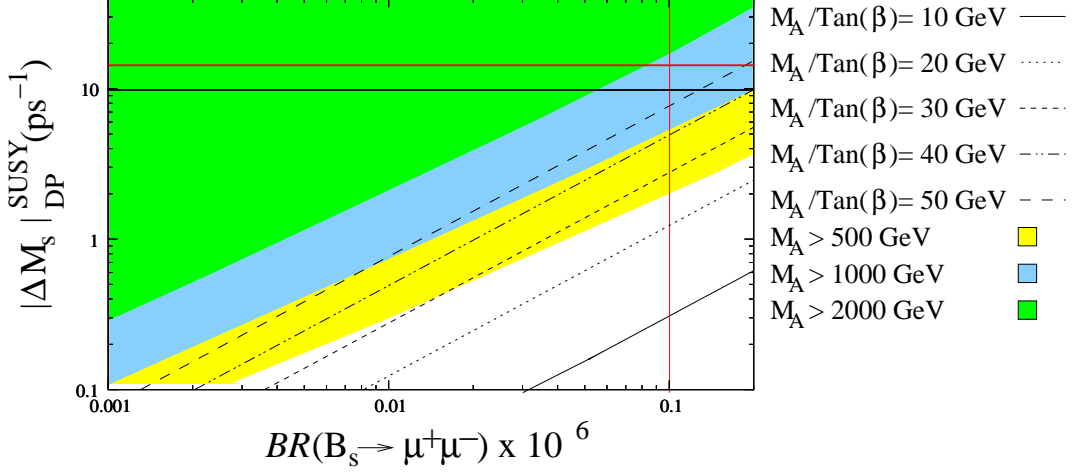


Figure 2: Correlation between $\mathcal{BR}(B_s \rightarrow \mu^+\mu^-)$ and ΔM_s . The squark masses are all uniform and have been set to 2 TeV. The rest of the SUSY parameters have been chosen so that $|\epsilon_0|$ and $|\epsilon_Y|$ have their maximal values. The black lines have fixed values of $M_A/\tan\beta$, but varying gluino phase. The contours represent ΔM_s for different ranges of M_A ($M_A \geq 500, 1000, 2000$ GeV) for gluino mass and A_t phases equal to π , and varying $\tan\beta$ values. The red (grey) vertical line is the experimental bound on $\mathcal{BR}(B_s \rightarrow \mu^+\mu^-)$. The horizontal black line is the 2σ upper bound on the double penguin contributions to ΔM_s from the UTfit group while red (grey) horizontal line is the same bound from the CKMfitter group.

where only the lowest order terms in (M_Z^2/M_A^2) have been kept. Using these tree-level approximations we find that

$$C_2^{LR} \propto \bar{m}_b \bar{m}_s \tan^4 \beta \frac{2}{M_A^2} \quad (76)$$

$$C_1^{SLL} \propto \bar{m}_b^2 \tan^2 \beta \frac{4M_Z^2}{M_A^4}. \quad (77)$$

Thus at large $\tan\beta$ and moderate or large M_A , C_2^{LR} clearly dominates over C_1^{SLL} .² The value of ΔM_s , including the corrections from new physics, may be represented as $(\Delta M_s)^{SM} |1 + f_s|$, where f_s is the total SUSY contribution. Due to C_2^{LR} being dominant we find

$$f_s = -\frac{16\pi^2 P_{LR}^2}{G_f^2 M_W^2 S_0(x_t) (V_{eff}^{32})^2} \frac{2}{M_A^2} (X_{RL}^A)^{32} (X_{LR}^A)^{32}. \quad (78)$$

In the limit of universal squark masses, for fixed values of the supersymmetry breaking mass parameters, the ratio between ΔM_s and $\mathcal{BR}(B_s \rightarrow \mu^+\mu^-)$ is proportional to

²When the loop factors and phases are included the approximation for C_1^{SLL} still holds up to a factor of order 1.

$(M_A/\tan\beta)^2$. Furthermore, f_s is negative [17, 18, 19]. Therefore, unless $|f_s| > 2$, the double penguin contributions to ΔM_s always interferes destructively with the SM contribution, at large $\tan\beta$. This result, showing the suppression of ΔM_s for enhanced $\mathcal{BR}(B_s \rightarrow \mu^+\mu^-)$, has been known for some time and was first shown in Ref. [17, 18, 19].

In Figs. 2 and 3 we show the correlation between ΔM_s and $\mathcal{BR}(B_s \rightarrow \mu^+\mu^-)$ for different squark spectra and gaugino phases. In Fig. 2 the black curves show the correlation between the double penguin contributions to ΔM_s and $\mathcal{BR}(B_s \rightarrow \mu^+\mu^-)$ for uniform squark masses ~ 2 TeV. We have chosen the uniform squark masses to be ~ 2 TeV so as to ensure that for $M_A \leq 1$ TeV the effective Lagrangian in Eq.(1) and Eq.(2) remains valid. Had we chosen squark masses of the order of 1 TeV, then the low-energy effective theory would break down for M_A close to 1 TeV, and a more detailed analysis of the ϵ_i 's momentum dependence would be required for these large values of M_A . Each of the black curves have different values of $M_A/\tan\beta$. The contours represent the maximal values of $|\Delta M_s|^{DP}$, for a given value of $\mathcal{BR}(B_s \rightarrow \mu^+\mu^-)$, and for a given range of values of M_A . Due to the fact that for fixed M_A , the ratio of $|\Delta M_s|^{DP}$ to $\mathcal{BR}(B_s \rightarrow \mu^+\mu^-)$ goes like $1/\tan^2\beta$, in order to maximize $|\Delta M_s|$ for any given value of $\mathcal{BR}(B_s \rightarrow \mu^+\mu^-)$ we need to minimize the value of $\tan\beta$. Inspection of the expressions given above shows that this may be achieved by choosing positive values of μ , $\arg(M_3) = \arg(A_t) = \pi$ and maximal values of $|\epsilon_0|$ and $|\epsilon_Y|$. In order to define the contours we have taken the values of the loop corrections given in Eq. (70). The horizontal black and red (grey) line corresponds to an upper bound on the largest possible contribution to ΔM_s from new physics using the 2σ values obtained by the UTFit and CKMfitter collaborations, Eq. (62) and Eq. (63), respectively. In order to get a precise evaluation of this bound, a complete fit to the flavor violating processes within the MSSM should be performed, something that is beyond the scope of this paper. However, since in this region of parameters the only relevant new flavor violating contributions are from the double penguin diagrams, we can make an estimate of this bound in the following way: From Eq. (62) or Eq. (63) we have a $2\text{-}\sigma$ range that goes from values consistent with the experimentally measured value up to values much larger than the measured values. Therefore the negative double penguin contribution can be as large as the difference between the maximum allowed SM value and the smallest allowed experimental value. This leads to an upper bound on the magnitude of the double penguin contributions to ΔM_s of about $\sim 10 \text{ ps}^{-1}$ for the UTFit limits in Eq. (62) or $\sim 14.5 \text{ ps}^{-1}$ for the CKMfitter limits in Eq. (63). From Fig. 2 it is clear that, for CP-odd Higgs masses below 1 TeV, this bound does not lead to any further constraint beyond the one already obtained by the non-observation of the branching ratio of the decay $B_s \rightarrow \mu^+\mu^-$.

It is possible to enhance the value of ΔM_s beyond what we have explored, by allowing values of $|\mu| > 2 m_{\tilde{q}}$. If, for instance, we consider values of $\mu \gtrsim 3m_{\tilde{q}}$, for the same value of $\mathcal{BR}(B_s \rightarrow \mu^+\mu^-)$ we can enhance ΔM_s by a factor ~ 1.5 . This suggests that the contours in Figs. 2 and 3 are not strict upper bounds, and can be further enhanced, almost in a linear way, by pushing $|\mu|/m_{\tilde{q}}$ to larger values. However, due to the extreme values of the mass parameters selected in defining the contours, these are indicative of the upper bound on the the double penguin contributions to ΔM_s for a given value of $\mathcal{BR}(B_s \rightarrow \mu^+\mu^-)$ for natural

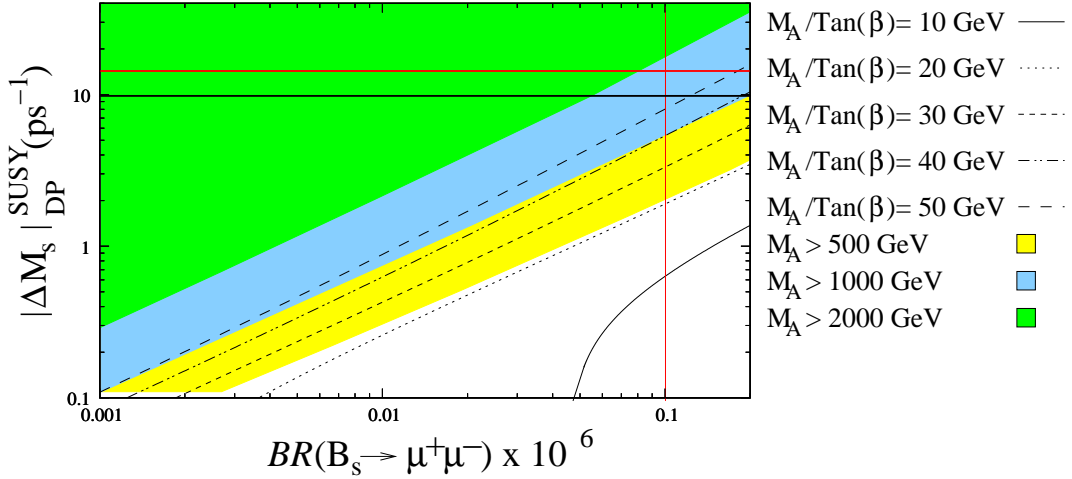


Figure 3: Same as Fig. 2, but for third generation soft supersymmetry breaking squark masses equal to 0.5 TeV and first and second generation squark masses equal to 5 TeV.

values of the mass parameters.

In Fig. 3 we depart from the limit of universal squark masses, by setting the third generation squark masses ~ 0.5 TeV while the first two generation squark masses are 5 TeV, which leads to ϵ_0^3 having its maximal value, but ϵ_0^1 and ϵ_0^2 being 100 times smaller. Hence, this splitting of the squark masses spoils the linear correlation between ΔM_s and $\mathcal{BR}(B_s \rightarrow \mu^+ \mu^-)$ due to the different parametric dependences of X_{RL}^{32} and X_{RL}^{23} for split masses. In both Figs. 2 and 3 the vertical red (grey) line is the experimental bound on $\mathcal{BR}(B_s \rightarrow \mu^+ \mu^-)$ in Eq. (66).

Figs. 2 and 3 suggest that large double penguin contributions to $|\Delta M_s|$ may not be obtained, for values of ϵ_0^J and ϵ_Y close to their maximal values in Eqs. (69) and (70), without violating the $\mathcal{BR}(B_s \rightarrow \mu^+ \mu^-)$ bound. Due to these bounds, for values of $M_A < 1$ TeV, the double penguin corrections to ΔM_s are restricted to be negative and relatively small, so that $|\Delta M_s|^{\text{SUSY}} \lesssim 4 \times 10^{-12}$ GeV, or equivalently $|\Delta M_s|^{\text{SUSY}} \lesssim 6$ ps $^{-1}$.

The $\mathcal{BR}(B_s \rightarrow \mu^+ \mu^-)$ bound also constrains contributions to ΔM_d and ΔM_K to values within experimental errors. For example, in Fig. 4, the SUSY contributions to ΔM_K in the Kaon system for uniform squarks masses are below the experimental error of 6×10^{-18} GeV or 0.01 ns $^{-1}$, even for large values of $(M_A / \tan \beta)^2$. These results seem to be at variance with those obtained in Ref. [20]. This is mainly due to the fact that the authors of Ref. [20] represented results in regions of parameters where the value of $\mathcal{BR}(B_s \rightarrow \mu^+ \mu^-)$ is well above the present limit. Observe that, to arrive at this conclusion, the new limit on $\mathcal{BR}(B_s \rightarrow \mu^+ \mu^-)$ is essential. From Fig. 4 we can also see how the improvement in the limit on $\mathcal{BR}(B_s \rightarrow \mu^+ \mu^-)$ forces the double penguin contributions to $|\Delta M_K|$ from SUSY to be small. Finally, Fig. 5 shows similar results for ϵ_K . As happens in the case of ΔM_K , the results for values of $M_A < 1$ TeV are far below the current experimental value of 2.282×10^{-3} .

However, within the Minimal Flavor Violation scheme, large contributions to ΔM_s are

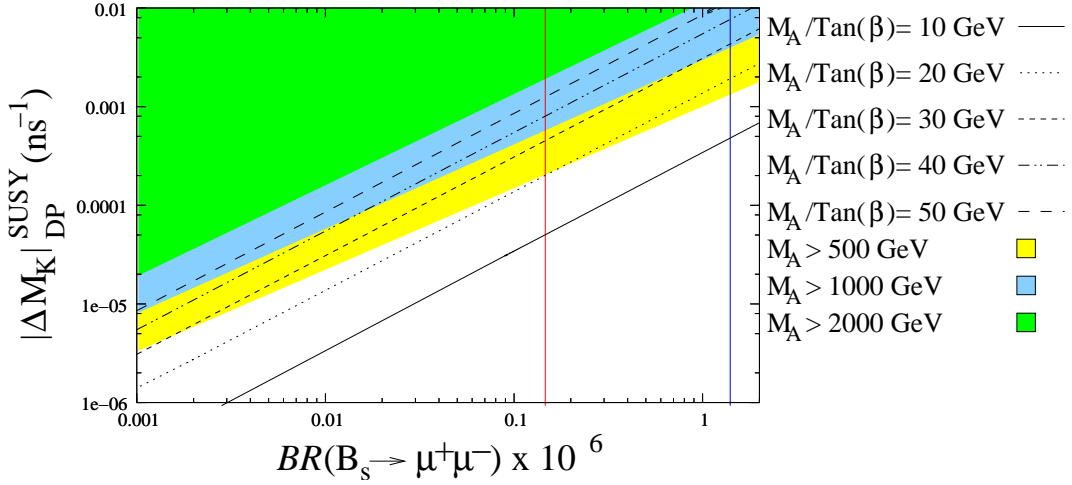


Figure 4: Correlation between $\mathcal{BR}(B_s \rightarrow \mu^+\mu^-)$ and ΔM_K . The squark masses are all uniform and have been set to 2 TeV. The rest of the SUSY parameters have been chosen so that $|\epsilon_0|$ and $|\epsilon_Y|$ have their maximal values. The black lines have fixed values of $M_A/\tan\beta$. The contours are the double penguin contributions to ΔM_K for gluino mass and A_t phases equal to π , but varying $\tan\beta$. The left red (grey) vertical line is the present experimental bound on $\mathcal{BR}(B_s \rightarrow \mu^+\mu^-)$ while the right blue (black) vertical line is the previous limit.

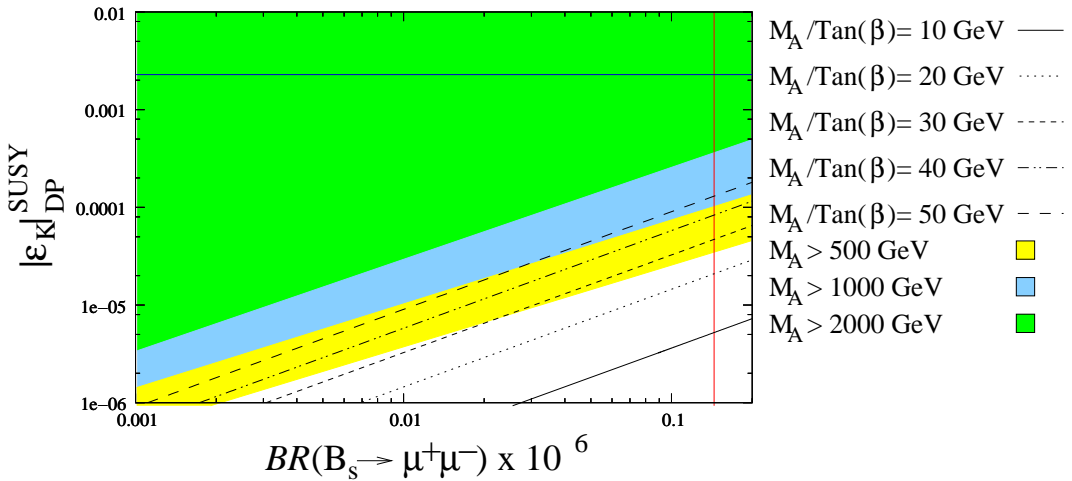


Figure 5: Same as Fig. 4, but for ϵ_K . Only the current bound on $\mathcal{BR}(B_s \rightarrow \mu^+\mu^-)$ is shown, by the vertical red (grey) line and the horizontal blue (black) line is the experimentally measured value of ϵ_K .

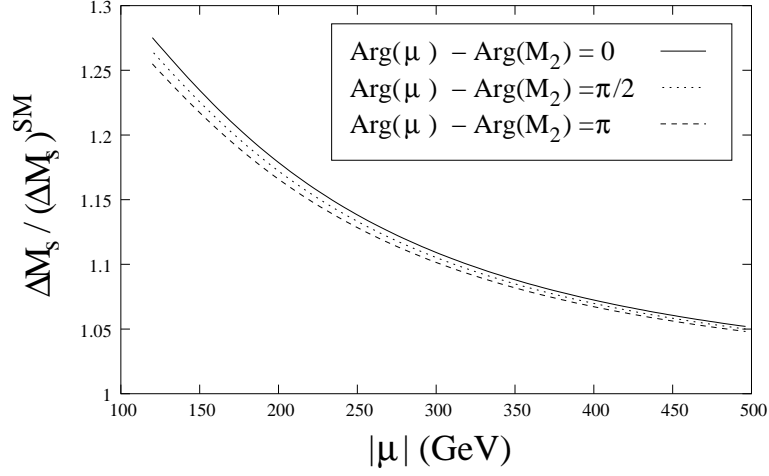


Figure 6: Variation of SUSY contributions to ΔM_s with input parameters $M_A = 200$ GeV, $M_3 = 1000$ GeV, $M_{D_3} = M_{SUSY} = 2000$ GeV, $2M_1 = M_2 = \mu$, $M_{U_3}^2 = -90^2$ GeV², $A_t = -1000$ GeV and $\tan \beta = 10$

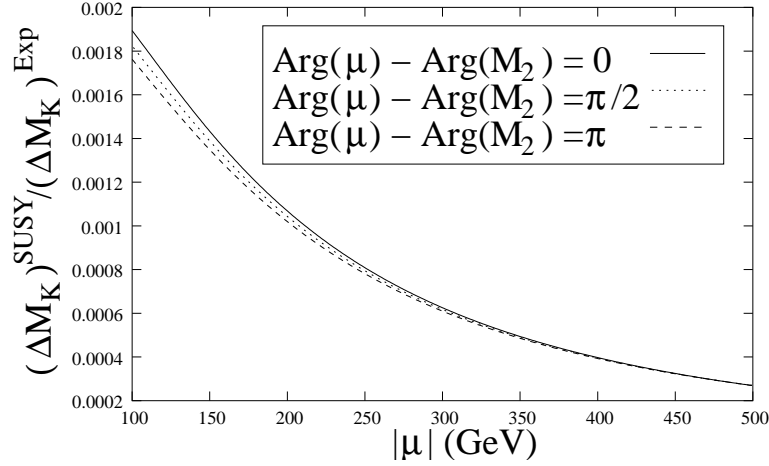


Figure 7: Variation of SUSY contributions to ΔM_K with input parameters $M_A = 200$ GeV, $M_3 = 1000$ GeV, $M_{D_3} = M_{SUSY} = 2000$ GeV, $2M_1 = M_2 = \mu$, $M_{U_3}^2 = -90^2$ GeV², $A_t = -1000$ GeV and $\tan \beta = 10$

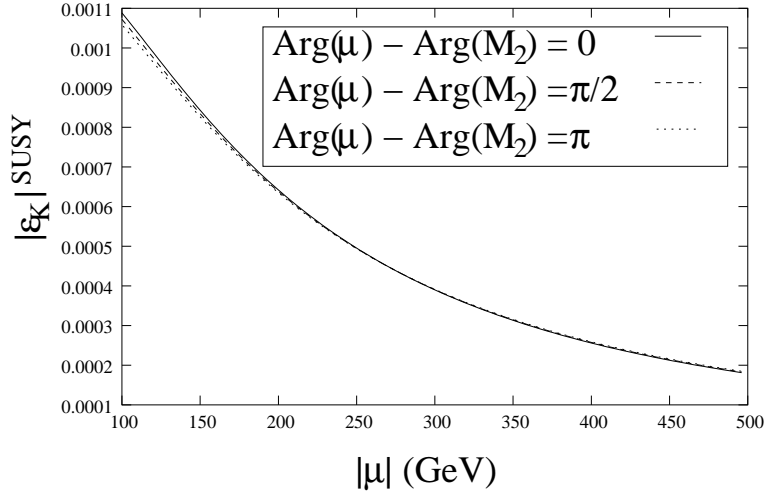


Figure 8: Variation of SUSY contributions to ϵ_K with input parameters $M_A = 200$ GeV, $M_3 = 1000$ GeV, $M_{D_3} = M_{SUSY} = 2000$ GeV, $2M_1 = M_2 = \mu$, $M_{U_3}^2 = -90^2$ GeV², $A_t = -1000$ GeV and $\tan\beta = 10$

possible for scenarios in which the stops and charginos are light, so that the chargino-stop box diagrams become larger. Furthermore, the bound on $\mathcal{BR}(B_s \rightarrow \mu^+ \mu^-)$ can be satisfied by going to regions of large M_A or low $\tan\beta$ as chargino-stop box contributions are not very sensitive to $\tan\beta$. This scenario is similar to that discussed in Ref. [29] where low values of $\tan\beta$ satisfy both the dark matter and baryogenesis constraints. In Fig. 6, we choose SUSY parameters

$$\begin{aligned}
 &M_A = 200 \text{ GeV}, M_3 = 1000 \text{ GeV}, M_{D_3} = M_{SUSY} = 2000 \text{ GeV}, \\
 &M_{U_3}^2 = -90^2 \text{ GeV}^2, A_t = -1000 \text{ GeV} \tan\beta = 10, \\
 &\text{and } 100 \text{ GeV} \lesssim 2M_1, M_2, \mu \lesssim 500 \text{ GeV}
 \end{aligned}$$

that agree with dark matter and baryogenesis constraints and produce a value of ΔM_s that is enhanced with respect to the SM value. For this kind of particle spectrum the double penguin contributions to ΔM_s are small compared to that of chargino stop diagrams. Although the enhancement of ΔM_s is small, a comparison of the SM prediction, Eq. (62) and Eq. (63), and the experimentally measured value leads to disfavor additional positive contributions of ΔM_s , larger than about 3.5 ps^{-1} , where we have taken into account the SM allowed range given by the CKMfitter collaboration Eq.(63), at the $2\text{-}\sigma$ level. Even stronger constraints would be obtained if the UTfit values in Eq.(63) for $(\Delta M_s)^{\text{SM}}$ were used. Therefore the smallest values of μ , smaller than 200 GeV, would be disfavored. A global fit to all flavor dependent observables within this scenario would be necessary in order to determine the precise lower bound on μ , something that is beyond the scope of this article. Also observe that for larger values of $\tan\beta$ there may be relevant double penguin contributions that could cancel the positive box-diagram contributions and therefore the bound on μ could be relaxed

in this case.

Although this scenario leads to contributions to ΔM_K that are smaller than the present experimental errors on this quantity, as can be seen in Fig. 7, it leads to interesting corrections to ϵ_K , as shown in Figure 8. The results in Fig. 8 were obtained for a value of the CKM phase $\delta = \pi/3$ (the best fit value within the SM). Experimentally we know that

$$|\epsilon_K| = (2.282 \pm 0.014) \times 10^{-3}. \quad (79)$$

and therefore the SUSY corrections are significant. For lower values of the CKM phase, however, the SUSY contributions to $|\epsilon_K|$ within this scenario can be smaller. The experimental value of ϵ_K is usually used to put a constraint on the $\bar{\rho} - \bar{\eta}$ plane³. The SM contributions to ϵ_K leads to the constraint equation [46]

$$5.3 \times 10^{-4} = B_K A^2 \bar{\eta} [(1 - \bar{\rho}) A^2 \lambda^4 \eta_2^* S(x_t^*) + \eta_3^* S(x_c^*, x_t^*) - \eta_1^* x_c^*] \quad (80)$$

where $B_K = 0.75 \pm 0.10$, $A \sim 0.85$, $\lambda = 0.22$, $\eta_1^* = 1.32_{-0.23}^{+0.21}$, $\eta_2^* = 0.57_{-0.01}^{+0.00}$, $\eta_3^* = 0.47_{-0.04}^{+0.03}$ and $S(x_t)$ and $S(x_c, x_t)$ are the Inami-Lim functions. Because the stops are light the dominant contributions to ϵ_K come from the chargino stop diagram. Under these approximations we find the ϵ_K constraint equation in $\bar{\rho} - \bar{\eta}$ plane is modified to become

$$5.3 \times 10^{-4} = B_K A^2 \bar{\eta} [(1 - \bar{\rho})(1 + \zeta) A^2 \lambda^4 \eta_2^* S(x_t^*) + \eta_3^* S(x_c^*, x_t^*) - \eta_1^* x_c^*]. \quad (81)$$

where ζ hides all the SUSY dependences. The dominant contribution to ϵ_K from SUSY comes from the C_{VLL} Wilson coefficient. Thus we have approximately,

$$\zeta \sim \frac{\bar{P}_{VLL}}{8G_F^2 M_W^2 S(x_t^*)} D_2(m_{\tilde{t}_2}^2, m_{\tilde{t}_2}^2, m_{\chi_2}^2, m_{\chi_2}^2) \quad (82)$$

where $m_{\tilde{t}_2}$ is the lightest stop mass, m_{χ_2} is the lightest chargino mass and D_2 is the Passarino-Veltmann function

$$D_2(x, y, z, t) = \frac{y^2}{(y-x)(y-z)(y-t)} \log\left(\frac{y}{x}\right) + \frac{z^2}{(z-x)(z-y)(z-t)} \log\left(\frac{z}{x}\right) + \frac{t^2}{(t-x)(t-y)(t-z)} \log\left(\frac{t}{x}\right). \quad (83)$$

Taking the lightest stop mass to be 120 GeV and approximating the the lightest chargino mass by $|\mu|$ we can estimate $\zeta \sim 0.4$ for values of $\mu \sim 100$ GeV. However as $|M_2| \simeq |\mu|$ there are also relevant contributions from the heavier chargino. Including these contributions, we obtain $\zeta \sim 0.55$. Including this value of ζ in the theoretical prediction for ϵ_K will lead to a modification of the values of $\bar{\rho}$ and $\bar{\eta}$ extracted from the fit to the flavor observables. Although a global fit to these quantities within the light stop scenario is beyond the scope of this article, we notice that for $\zeta \lesssim 0.55$, the new constraint equation, Eq. (81), is still consistent with the limits coming from $|V_{ub}|/|V_{cb}|$, $\sin(2\beta)_{\text{eff}}$ and $\Delta M_{s,d}$ and therefore this scenario is not ruled out by these considerations.

³ $\bar{\rho}$ and $\bar{\eta}$ are the usual corrected Wolfenstein parameters of the CKM matrix

4.1.2 The effect of $\mathcal{BR}(B_s \rightarrow \mu^+\mu^-)$ constraint on Higgs physics at the Tevatron and the LHC

As shown above, in the minimal flavor violating scheme, all dominant FCNC effects at large $\tan\beta$ are proportional to ϵ_Y , which is directly proportional to the product of the μ and A_t , but inversely proportional to the square of the squark masses. The FCNC effects are strongly enhanced for large values of $\tan\beta$ and small values of the CP-odd Higgs mass. The Tevatron collider is performing searches for non-standard Higgs bosons, which become efficient for exactly the same conditions. Therefore, in minimal flavor violating models, current bounds on the rate $B_s \rightarrow \mu^+\mu^-$ impose strong constraints on the possibility of finding non-standard Higgs bosons at the Tevatron collider (for related studies, see Refs. [57]–[59]). This is particularly true for large values of the A_t and μ parameters, for which ϵ_Y is enhanced.

Low values of the CP-odd Higgs mass are also associated with low values of the charged Higgs mass. These values of the charged Higgs mass induce large positive corrections to the branching ratio $BR(b \rightarrow s\gamma)$. Since the measured value of $BR(b \rightarrow s\gamma)$ agrees well with the SM prediction, these large charged Higgs induced corrections to the rare decay rate needs to be cancelled by similarly large corrections induced by supersymmetric particles. In minimal flavor violating schemes, these SUSY corrections are associated with stop-chargino loops [14],[48]–[53]. For positive (negative) values of $A_t\mu$, the corrections to the amplitude of the decay $b \rightarrow s\gamma$ have the same (opposite) sign to the ones associated with the charged Higgs corrections, and grow linearly with $\tan\beta$. Therefore, agreement of the theoretical predictions with the experimental values of $BR(b \rightarrow s\gamma)$ for small values of M_A demands negative values of $A_t\mu$.

Additional constraints come from the CP-even Higgs sector. For a given value of the overall squark masses, the mass of the lightest CP-even Higgs boson in the large $\tan\beta$ regime depends strongly on the parameter A_t . In particular, this mass is maximized for a value of $X_t = A_t - \mu/\tan\beta \simeq 2.4 M_{SUSY}$ (where M_{SUSY} is equal to the average stop mass) and minimized for values of $X_t = 0$ [3]. Due to the complicated dependence of the Higgs boson properties on the supersymmetric mass parameters, searches for Higgs bosons at the Tevatron and the LHC are usually interpreted in terms of benchmark scenarios [47]. For instance, the scenario with $X_t/M_{SUSY} \simeq 2.4$ is named the maximal mixing scenario, since it is associated with the values of the stop mixing parameters that maximize the lightest CP-even Higgs mass. Similarly, $X_t = 0$ defines the minimal mixing scenario. While for the maximal mixing scenario the constraints coming from FCNC are particularly strong, no constraint from $B_s \rightarrow \mu^+\mu^-$ are expected to be obtained in the minimal mixing scenario.

In Fig. 9, we display the constraints in the M_A – $\tan\beta$ plane that are induced by the requirement of obtaining a good agreement with the $BR(b \rightarrow s\gamma)$ and the non-observation of $B_s \rightarrow \mu^+\mu^-$ at the Tevatron collider. The results are presented for different values of X_t and μ parameters and supersymmetry breaking squark masses equal to 1 TeV. The region of parameter space consistent with $B_s \rightarrow \mu^+\mu^-$ for $\mu = -100$ GeV and $\mu = -200$ GeV is below the dotted and dashed lines respectively. For each value of A_t , larger values of $|\mu|$ imply consistency with larger values of M_A and smaller values of $\tan\beta$. On the other hand,

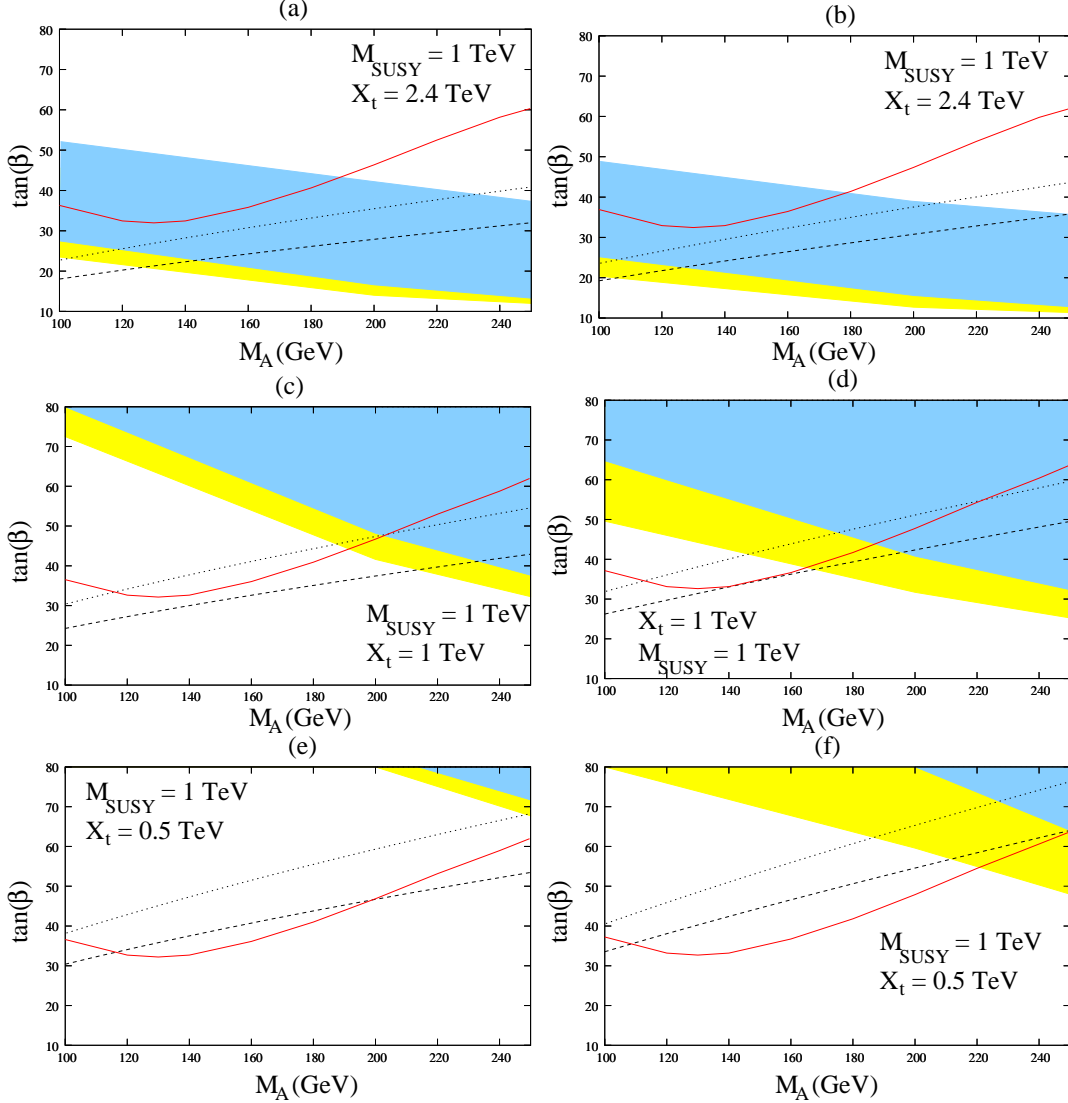


Figure 9: The dashed(dotted) line is the $\mathcal{BR}(B_s \rightarrow \mu^+\mu^-)$ experimental bound in the $M_A - \tan\beta$ plane for $\mu = -200(-100)$ GeV and the yellow (light grey) and blue (dark grey) bands are the $b \rightarrow s\gamma$ allowed regions for $\mu = -200$ GeV and -100 GeV, respectively, in the uniform squark limit with $M_{\text{SUSY}} = 1$ TeV, $|M_3| = 0.8$ TeV, and $2M_1 = M_2 = 110$ GeV. The red (grey) line is the projected CDF limit on $H \rightarrow \tau\tau$ for 1fb^{-1} luminosity. Larger luminosities would probe larger M_A and smaller $\tan\beta$. Also changing μ from -200 GeV to -100 GeV does not affect the CDF limit significantly. Figures (a),(c) and (e) have different values of $X_t = A_t - \mu/\tan\beta$ for $\arg(M_3) = 0$ while (b), (d) and (f) have a $\arg(M_3) = \pi$

the regions in the $M_A - \tan \beta$ plane that are consistent with the observed values of

$$BR(b \rightarrow s\gamma)^{Exp} = 3.38_{-0.28}^{+0.3} \times 10^{-4} \quad (84)$$

and the estimated theoretical uncertainty [54]

$$|BR(b \rightarrow s\gamma)^{Exp} - BR(b \rightarrow s\gamma)^{SM}| < 1.3 \times 10^{-4} \quad (85)$$

are given by the colored bands. For larger values of $|\mu|$ the bands move to smaller values of M_A or smaller values of $\tan \beta$. Actually, the approximate cancellation of the charged Higgs and chargino stop contributions implies a correlation between $1/M_A^2$ and $A_t \mu \tan \beta$. We have also plotted the projection of the CDF limit for non-standard MSSM Higgs boson inclusive searches in the $A, H \rightarrow \tau\tau$ channel for a total integrated luminosity of 1 fb^{-1} . In order to obtain this limit we have used the approximate relation given in Ref. [55]

$$\sigma(gg, b\bar{b} \rightarrow A) \times \mathcal{BR}(A \rightarrow \tau^+\tau^-) \sim \sigma(gg, b\bar{b} \rightarrow A)_{SM} \frac{\tan^2 \beta}{(1 + \epsilon_3 \tan \beta)^2 + 9}, \quad (86)$$

along with the Tevatron's reach for scenario of maximal mixing with $\mu \sim -200 \text{ GeV}$ and a luminosity of 1 fb^{-1} shown in Ref. [56].

The Tevatron collider is only sensitive to values of M_A smaller than about 300 GeV and values of $\tan \beta$ larger than about 40. For maximal mixing, Fig. 9(a) shows that the constraints coming from flavor physics are sufficiently strong so as to restrict the parameter space consistent with the search for non-standard Higgs bosons at the Tevatron collider. On the other hand, for values of $A_t \simeq 1 \text{ TeV}$, Fig. 9(c) shows that one can obtain borderline consistency with the constraints coming from the flavor sector, but only for the smaller values of μ and $M_A \simeq 200 \text{ GeV}$. Finally, for values of $A_t = 500 \text{ GeV}$ or smaller, Fig. 9(e) shows that the bounds coming from $BR(b \rightarrow s\gamma)$ are sufficiently strong as to strongly restrict the parameter space consistent with non-standard Higgs boson searches at the Tevatron collider.

The situation is ameliorated for positive values of μM_3 , keeping negative values of μA_t . In Figs. 9(b),(d) and (f) we have changed the sign of the gluino mass (the same results would be obtained by keeping the gluino mass fixed but changing the sign of μ and A_t). Positive values of μM_3 diminish the ϵ_0 contributions and hence make the bound coming from $\mathcal{BR}(B_s \rightarrow \mu^+\mu^-)$ slightly less severe. The bound coming from $\mathcal{BR}(b \rightarrow s\gamma)$ is also improved, with the colored bands being slightly lower. Thus for $X_t \lesssim 1 \text{ TeV}$ the region of $M_A \sim 200 \text{ GeV}$, small μ and $\tan \beta \sim 50$, that is not excluded by flavor physics, will be probed by the Tevatron Higgs searches in the near future.

Finally, we consider the minimal mixing scenario, $X_t \simeq 0$. In this case, the constraints coming from the non-observation of $B_s \rightarrow \mu^+\mu^-$ become very weak, even for large values of $|\mu|$. As we will explain below, this opens up an interesting possibility: The dominant charged Higgs contribution to the $b \rightarrow s\gamma$ amplitude at large $\tan \beta$ is proportional to the charged Higgs coupling to top and bottom quarks given in Eq. (44). Setting, for simplicity, $A_b = 0$ makes the $\epsilon'_Y \approx 0$ while

$$\epsilon'_0 \approx \frac{2\alpha_s}{3\pi} \mu M_3 (\cos^2 \theta_i C_0(m_{\tilde{s}_L}^2, m_{\tilde{t}_1}^2, M_3^2) + \sin^2 \theta_i C_0(m_{\tilde{s}_L}^2, m_{\tilde{t}_2}^2, M_3^2)). \quad (87)$$

Therefore, in this case, the charged Higgs contribution to the $\mathcal{BR}(b \rightarrow s\gamma)$ becomes proportional to [50, 51]

$$A_{H^+} \propto \frac{1 - \frac{2\alpha_s}{3\pi} \mu M_3 \tan \beta \left(\cos^2 \theta_{\tilde{t}} C_0(m_{\tilde{s}_L}^2, m_{\tilde{t}_1}^2, M_3^2) + \sin^2 \theta_{\tilde{t}} C_0(m_{\tilde{s}_L}^2, m_{\tilde{t}_2}^2, M_3^2) \right)}{1 + \epsilon_3 \tan \beta}, \quad (88)$$

where $\theta_{\tilde{t}}$ is the stop mixing angle. From Eq. (88) we can clearly see that for large positive values of $M_3\mu$ and $\tan \beta$, the charged Higgs amplitude can be strongly reduced. Furthermore when $X_t \simeq 0$ the chargino stop contribution to $b \rightarrow s\gamma$ is also small. Since, for these parameters, the BSM contributions to the $\mathcal{BR}(b \rightarrow s\gamma)$ are small, the experimental limit in Eq. (84) puts only a weak constraint on the allowed value of M_A . Moreover, as stressed above, for this parameter region $B_s \rightarrow \mu^+\mu^-$ also provides no constraint because $X_t \sim 0$ implies small values of ϵ_Y .

Additionally, for the values of the parameters for which a cancellation of the charged Higgs contribution to $BR(b \rightarrow s\gamma)$ occurs, the usual bound on $\tan \beta$ that comes from requiring that y_b be perturbative up to the GUT scale may be relaxed: The bottom Yukawa has the form

$$y_b \simeq \frac{\sqrt{2}m_b \tan \beta}{v(1 + \epsilon_3 \tan \beta)} \quad (89)$$

and as $\epsilon_3 \tan \beta$ is real and positive, and of order one for the cancellation to occur, the denominator suppresses the Yukawa for large values of $\tan \beta$. This leads to an enhancement of the upper bound on $\tan \beta$ coming from perturbative consistency in the bottom quark sector.

In Fig. 10 we illustrate such a scenario for different values of $|\mu|$. Because both the $B_s \rightarrow \mu^+\mu^-$ and $b \rightarrow s\gamma$ constraints allow essentially any value of $M_A \gtrsim 100$ GeV a large region of the $M_A - \tan \beta$ can be probed by the heavy MSSM Higgs searches at the Tevatron. Interestingly enough, the lightest Higgs boson mass is also close to the experimental bound $m_h \simeq 115$ GeV in this region of parameters, and therefore it could be at the reach of the Tevatron collider searches.

In conclusion, for minimal flavor violating schemes, the discovery of a non-standard Higgs signature at the Tevatron collider would point to a definite region of parameter space, with values of X_t of order of the squark masses or smaller. Larger values are strongly restricted by the present Tevatron, CLEO and B-factory experimental constraints. It is important to remark that, as the luminosity of the Tevatron increases, the probability of measuring $B_s \rightarrow \mu^+\mu^-$ increases, and so does the one of measuring a non-standard Higgs boson signal. However, as it becomes clear from the above discussion, an improvement of the bound on $B_s \rightarrow \mu^+\mu^-$ would put strong restrictions on the possibility of measuring a non-standard Higgs boson signature for moderate or large values of X_t . Conversely, if a Higgs boson signature were observed, with absence of observation of $B_s \rightarrow \mu^+\mu^-$, it would imply either small values of X_t , or a strong departure from minimal flavor violating scenarios.

It is interesting to analyze the constraints that the non-observation of $B_s \rightarrow \mu^+\mu^-$ at the LHC, for a total integrated luminosity of order of 10 fb^{-1} , would put on the MSSM

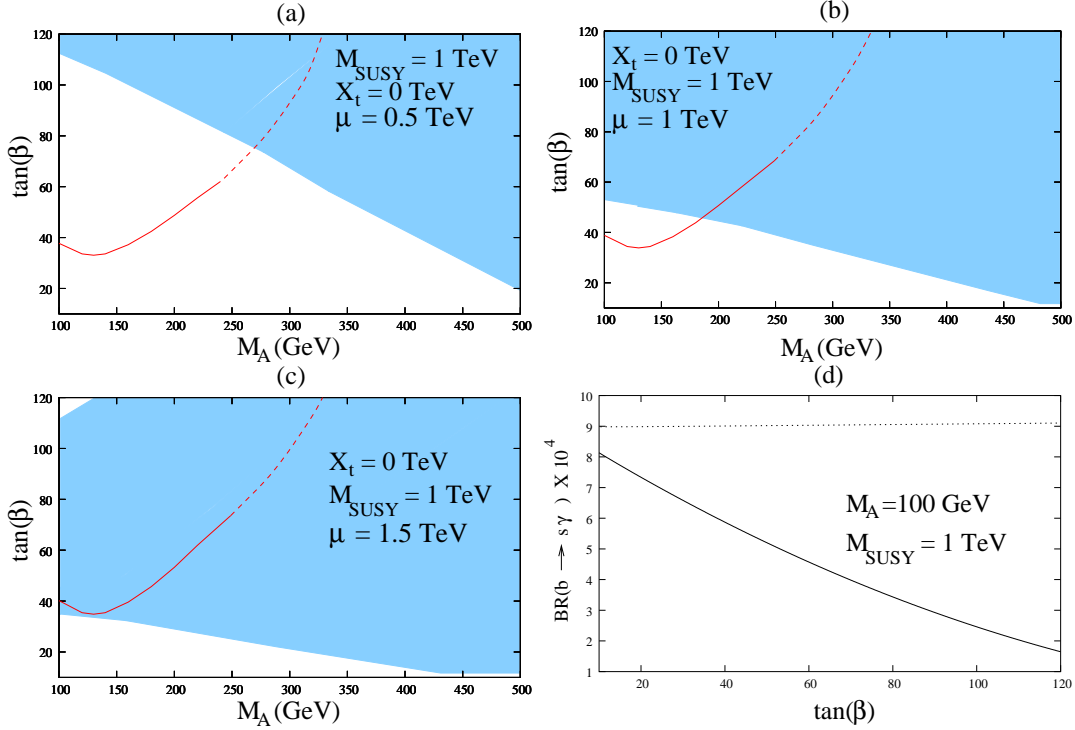


Figure 10: (a)–(c) Corresponds to $\mu = 500 - -1500$ GeV with the blue (dark grey) band showing $b \rightarrow s\gamma$ allowed regions for these values of μ in the uniform squark mass limit with a common value of the squark masses $M_{\text{SUSY}} = 1$ TeV, $M_3 = 0.8$ TeV, $2M_1 = M_2 = 110$ GeV. The red (grey) line is the projected CDF limit on $H \rightarrow \tau\tau$ for 1fb^{-1} luminosity. The dashed part of the projected Tevatron reach is an extrapolation of the curve. (d) Shows the effect of including the squark loop correction to $P_{RL}^{H^+}$ vertex, proportional to $\epsilon_0^{3'}$, on $b \rightarrow s\gamma$ rate for $\mu = 1$ TeV. The dashed line corresponds to the case when corrections are not included while the solid line corresponds to the case when they are included.

parameter space. The projected Atlas bound on $BR(B_s \rightarrow \mu^+\mu^-)$ in this case would be of order $5.5 \cdot 10^{-9}$ [60], and therefore would imply strong constraints on the M_A - $\tan\beta$ parameter space (The final Tevatron bound, in case of non-observation of $B_s \rightarrow \mu^+\mu^-$, assuming a total integrated luminosity of order 8fb^{-1} , will be close to $2 \cdot 10^{-8}$ [61] and therefore it will set similarly strong bounds on the parameter space). In order to study the possible implications for searches of non-standard Higgs bosons at the LHC, we have considered the projected reach of the CMS searches in the inclusive $pp \rightarrow \Phi + X$, $\Phi \rightarrow \tau^+\tau^-$ mode, at a luminosity of 30fb^{-1} [62].

From Fig. 11 we can see that even for the most restrictive case of maximal mixing and negative values of μM_3 , the bound coming from the non-observation of $B_s \rightarrow \mu^+\mu^-$ would be consistent with the observation of a non-standard Higgs boson for small values of $|\mu| \simeq 100$ GeV and somewhat large values of $350 \lesssim M_A \lesssim 500$ GeV. These bounds are

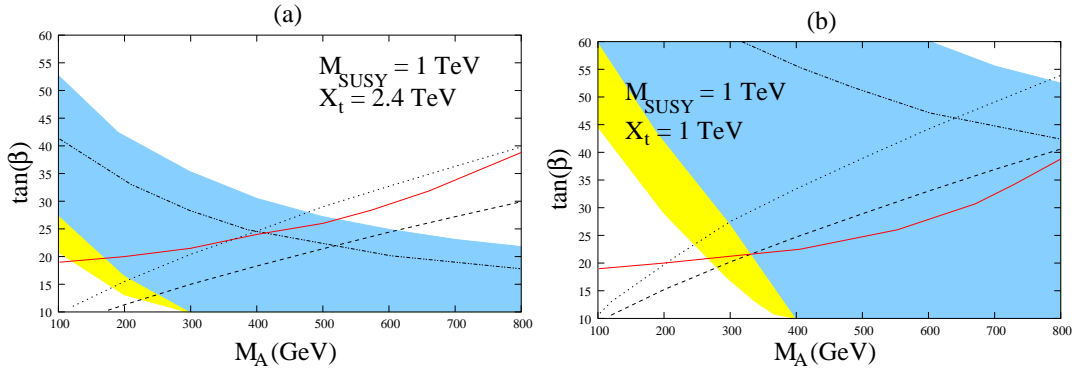


Figure 11: Comparison of the projected reach for non-standard Higgs bosons at the LHC in the inclusive $pp \rightarrow \Phi + X$, $\Phi \rightarrow \tau^+\tau^-$ mode (red (grey) line) with the limits that would be obtained in case of non-observation of the decay mode $B_s \rightarrow \mu^+\mu^-$ for an integrated luminosity of 10 fb^{-1} for $\mu = -100 \text{ GeV}$ (dotted line) and $\mu = -300 \text{ GeV}$ (dashed line). Blue (dark grey) and yellow (light grey) areas correspond to the bounds coming from $BR(b \rightarrow s\gamma)$ for $\mu = -100 \text{ GeV}$ and $\mu = -300 \text{ GeV}$, respectively. The upper edge of the $\mu = -300 \text{ GeV}$ area is denoted by the dot-dashed line. We show these results for a common value of the squark masses $M_{\text{SUSY}} = 1 \text{ TeV}$ and (a) $X_t = 2.4 \text{ TeV}$, (b) $X_t = 1 \text{ TeV}$, and positive (negative) values of μM_3 (μA_t), and $|M_3| \simeq 0.8 \text{ TeV}$.

strongly relaxed for smaller values of X_t . For instance, for $X_t \lesssim 1 \text{ TeV}$, observation of non-standard Higgs bosons would be still allowed for any value of M_A , provided $|\mu| \lesssim 300 \text{ GeV}$.

5 Non-minimal Flavor Violation

5.1 Gluino Contributions to ΔM_s

The results in the case of non-minimal flavor violation discussed in section 2.1.2 are quite similar to the case of minimal flavor violation. As in the case of MFV for large $\tan\beta$, the dominant contribution to ΔM_s comes from the DP diagrams. However, in the non-minimal flavor violation scenario introduced here, the effects of gluino boxes can also be important and compete with the double penguin contributions. The appearance of the gluino-box contributions is a direct consequence of the quark-squark-gluino vertices not being diagonal in the flavor basis. In the case of uniform squarks masses these contributions disappear due to the CKM matrix being unitary.

The double penguin contributions to $\mathcal{BR}(B_s \rightarrow \mu^+\mu^-)$ in the non-minimal flavor scenario may be significantly larger than in the case of MFV. For instance, assuming that the third generation left-handed and right-handed down squark masses are light implies that the

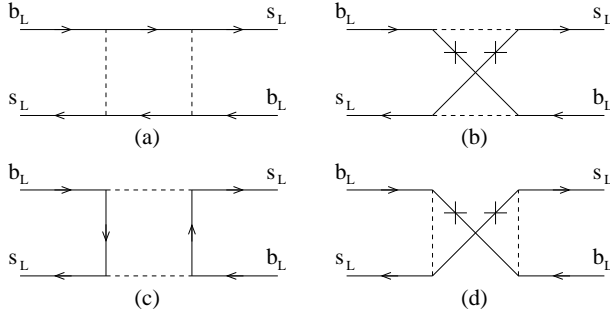


Figure 12: Gluino box diagrams that make contributions to ΔM_s for the Nonminimal flavor violation. Diagrams (b) and (d) are possible because the gluinos are Majorana and the lower diagrams have a relative sign difference with respect to the upper ones [63]

vertices in Eq. (25) are proportional to

$$X_{RL}^{JI} \propto V_{eff}^{3J*} V_{eff}^{3I} \left(\left(1 - \frac{1}{\rho^2} \right) \epsilon_0^3 + \epsilon_Y \right) \quad (90)$$

where $\rho = m_{\tilde{q}_{1,2}}/m_{\tilde{q}_3}$. Therefore when the squark mass splitting is large these vertices can give large contributions to ΔM_s and $\mathcal{BR}(B_s \rightarrow \mu^+ \mu^-)$. However, the linear correlation between ΔM_s and $\mathcal{BR}(B_s \rightarrow \mu^+ \mu^-)$ is not spoiled by the splitting of the squark masses as there is no flavor dependence in the factor multiplying $m_{d_J} V_{eff}^{3J*} V_{eff}^{3I}$ in Eq.(25). Therefore the $\mathcal{BR}(B_s \rightarrow \mu^+ \mu^-)$ bound is still a severe constraint on large double penguin contributions to ΔM_s like in the MFV scenario.

An interesting case is one in which the gluino box diagrams dominate over the double penguin contributions to ΔM_s for moderate values of $\rho \sim 2$ or 3. Similar to the light-stop scenario for MFV there are situations in which the gluino box diagram contributions are sizeable and the other contributions are suppressed. The double penguin contributions are suppressed for low values of $\tan \beta$. On the other hand, large values of μ and M_2 suppress the stop-chargino box diagrams. Since the gluino box diagram effects are larger for small values of the left-handed squark and gluino masses, we shall investigate the case in which the third generation left-squark soft supersymmetry breaking parameters are about 100 GeV. To avoid the Tevatron bound on sbottoms we also assume that the lightest neutralino is within 20 GeV of the sbottom mass [64]. We can achieve this mass difference by choosing an appropriate value of M_1 . For larger values of the soft SUSY breaking sbottom mass parameter, of about ~ 200 GeV the gluino box contribution becomes negligible.

Light left-handed squarks tend to lead to large values of the T -parameter and hence are constrained by precision electroweak data. These large contributions to the T -parameter are induced by the large difference between the left-handed sbottom and stop masses and are proportional to the top quark mass. However, for some range of values of the right-handed stop mass parameter, these large contributions may be minimized. Indeed, for large values of

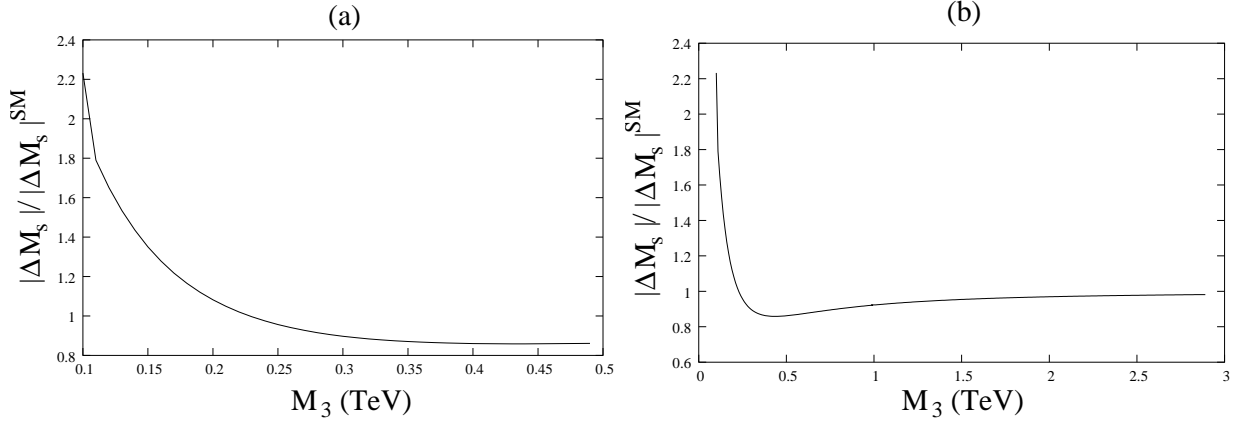


Figure 13: Variation of SUSY contributions to ΔM_s with input parameters $M_A = 250$ GeV, $M_{SUSY} = 1000$ GeV, $M_1 = 110$ GeV $M_2 = 1000$ GeV, $\mu = 1100$ GeV, $M_{(\tilde{U}_L, \tilde{D}_L)_{12}} = M_{\tilde{U}_R, \tilde{D}_R} = 1000$ GeV, $M_{(\tilde{U}_L, \tilde{D}_L)_3} = 100$ GeV, $A_t = 1110$ GeV, $\tan\beta = 10$ and all relevant SUSY phases are zero. (a) Shows the variation of ΔM_s over small values of gluino mass, while (b) shows that in limit of large gluino mass we recover the SM value.

the right handed stop mass parameter $M_{\tilde{U}_R}$ and $X_t \simeq M_{\tilde{U}_R}$, the lightest stop mass becomes mainly left-handed and its mass is given by

$$m_{t_1}^2 \simeq M_{\tilde{U}_L}^2 + m_t^2 \left(1 - \frac{X_t^2}{M_{\tilde{U}_R}^2} \right) + D_L^t \quad (91)$$

where D_L^t is the small D-term contribution to the left-handed stop mass. Observe that for $X_t \simeq M_{\tilde{U}_R}$, the top-quark mass contribution is strongly suppressed and hence the contribution to the T -parameter becomes small [65]. In our analysis we have chosen the stop mass parameters so that the relation $X_t = M_{\tilde{U}_R}$ is fulfilled.

In Fig.13 we see that for gluino masses below 200 GeV, the gluino-sbottom box contribution yields a value of ΔM_s that is greater than the 1σ bound coming from the SM. Similarly, in Fig. 14 we see that there are large negative contributions to ϵ_K from the gluino box-diagrams for $M_3 \lesssim 200$ GeV. The total value ΔM_s drops below that of the SM, for $M_3 \gtrsim 200$ GeV, because of the interference between the diagrams in Fig. 12. For the region $M_3 \lesssim 200$ GeV, where ΔM_s is large, the contributions to ϵ_K are also larger but negative, which seems to predict a total value of ϵ_K much smaller than the experimentally observed one. Therefore, the gluino box contributions to ΔM_s , in this non-minimal flavor violating scenario with flavor changing effects induced by the CKM matrix elements, are generally small and are at most as large as those in the light stop scenario discussed above. In addition this scenario is in general highly contrived as the experimental constraints from light gluino and sbottom searches [64] can be avoided only by going to a small corner of the MSSM parameter space.

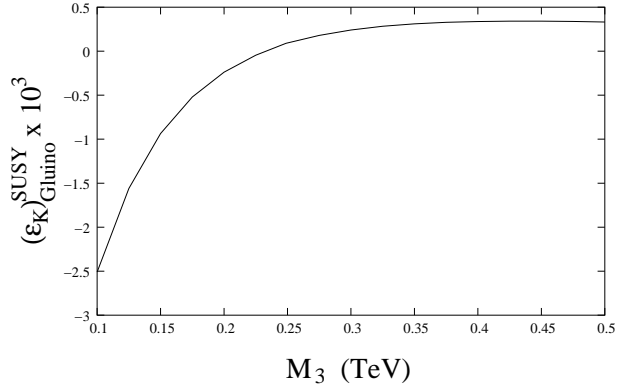


Figure 14: Variation of the gluino contributions to ϵ_K with the gluino mass M_3 for the same input parameters as in Fig. 13

6 Conclusions

In this article, we have studied the constraints on the parameter space of minimal flavor violating SUSY models coming from the latest constraints on $B_s \rightarrow \mu^+ \mu^-$, ΔM_s , ϵ_K and $BR(b \rightarrow s\gamma)$. Firstly, we have shown that the analysis of the double penguin contributions to observables in the Kaon sector could not be done with the available formulae in the literature. We derived a new formula that describes well the Kaon sector contributions and show that the present constraints on $B_s \rightarrow \mu^+ \mu^-$ eliminate the possibility of inducing relevant double penguin corrections in this sector. Alternative contributions, coming from chargino and stop loop corrections can produce large contributions to ϵ_K , which, considering the present theoretical uncertainties, are consistent with the bounds coming from other flavor observables.

We have also verified that the double penguin contributions to ΔM_s interfere destructively with the SM contribution and are strongly constrained by the non-observation of $B_s \rightarrow \mu^+ \mu^-$ at the Tevatron collider. Analyzing the dependence of ΔM_s on the supersymmetric loop corrections, we obtained upper bounds on this quantity for any given value of $B_s \rightarrow \mu^+ \mu^-$, for natural values of the supersymmetric mass parameters. We have also shown that for $M_A < 1$ TeV, under the current theoretical and experimental uncertainties, this bound is stronger than the bound on the new physics contributions that is obtained from the comparison of the SM predictions and the experimentally measured values. Finally, if the theoretical errors on ΔM_s were reduced and the SM central value was to remain the same then negative corrections to ΔM_s , like that of the double penguin contribution, would be necessary. However such double penguin corrections to ΔM_s of about a few ps^{-1} 's can be obtained only if $\mathcal{BR}(B_s \rightarrow \mu^+ \mu^-) \gtrsim 3 \times 10^{-8}$ for $M_A \leq 1$ TeV, which is within the future sensitivity of the Tevatron collider.

On the other hand, relevant, positive contributions to ΔM_s may be obtained for light stops and charginos. The contributions may be as large as 25 percent of the SM values,

almost independently of the value of $\tan\beta$. Contrary to the double penguin contribution, the chargino-stop contributions are positive and they are more strongly constrained than the negative double penguin ones. Small values of the Higgsino mass, $\mu < 200$ GeV tend to be disfavored for mass parameters consistent with the scenario of electroweak baryogenesis. We have also analysed a scenario in which there are flavor violating effects proportional to CKM matrix elements in the left-handed down squark-gluino vertices at tree-level. Although the box-diagrams may lead to significant contributions to ΔM_s for sufficiently small gluino and down squark masses, this contributions are constrained to be small once the bounds on ϵ_K are taken into account.

We have also analyzed the complementarity of these FCNC constraints with direct Tevatron searches for heavy MSSM Higgs bosons. We have analyzed different scenarios and showed that $\mathcal{BR}(b \rightarrow s\gamma)$ and $\mathcal{BR}(B_s \rightarrow \mu^+\mu^-)$ puts strong constraints on the $M_A - \tan\beta$ plane. This study suggests that within minimal flavor violating scenarios, the observation of non-standard MSSM Higgs bosons at the Tevatron collider would imply either moderate values of $|X_t/M_{SUSY}| \lesssim 1$ and small values of $|\mu|$, or very small values of X_t and large values of $|\mu|$. Interestingly enough, for values $X_t \lesssim M_{SUSY}$, the lightest CP-even Higgs boson mass is smaller than 120 GeV and therefore possibly at the reach of Tevatron high luminosity searches.

Finally, we have analysed the implications of non-observation of $B_s \rightarrow \mu^+\mu^-$ at the LHC, for a total integrated luminosity of order of 10 fb^{-1} , on searches for non-standard MSSM Higgs bosons at this collider. Even for the most restrictive case of maximal mixing and negative values of μM_3 , this situation would be consistent with the observation of a non-standard Higgs boson for small values of $|\mu| \simeq 100$ GeV and somewhat large values of $350 \lesssim M_A \lesssim 500$ GeV. For $X_t \lesssim 1$ TeV, instead, observation would be still allowed for any value of M_A , provided $|\mu| \lesssim 300$ GeV.

Acknowledgements: We wish to thank Csaba Balasz, Jon Rosner, Ishai Ben-Dov, Thomas Becher, Avto Kharchilava, Steve Mrenna, Jae Sik Lee and Ulrich Nierste for helpful discussions. R.N.-P and A.S. thank the Fermilab Theory Group for warm hospitality and support. Work at ANL is supported in part by the US DOE, Div. of HEP, Contract W-31-109-ENG-38. Fermilab is operated by Universities Research Association Inc. under contract no. DE-AC02-76CH02000 with the DOE. This work was also supported in part by the U.S. Department of Energy through Grant No. DE-FG02-90ER40560.

A Appendix

A.1 A corrected perturbative approach for calculating FCNC

We would like to develop a perturbative approach to calculating flavor changing vertices which in the limit of uniform $\hat{\epsilon}_0$ should reproduce the exact result in Eq. (27).

A.1.1 Basic setup and notation

As a starting point, we assume the form of the mass matrix

$$(\mathbf{M}_d)^{JI} = m_{d_J} \left((1 + \epsilon_J \tan \beta) \delta^{JI} + \epsilon_Y y_t^2 \tan \beta \lambda_0^{JI} \right). \quad (92)$$

As the off-diagonal elements are suppressed by CKM factors with respect to the diagonal elements we expand in terms of the CKM factors. Therefore first order terms are proportional to V_0^{3J} for $J \neq 3$ and second terms are proportional to $V_0^{*32} V_0^{31}$. Strictly speaking we should probably expand in the Wolfenstein parameter λ and not in the CKM elements, however as all we want is the leading behaviour, it is sufficient to expand in terms of the CKM elements. So \mathbf{M}_d has both first and second order terms present and can be expanded to be

$$\mathbf{M}_d = (\mathbf{M}_d)_0 + \delta \mathbf{M}_d + \delta^2 \mathbf{M}_d. \quad (93)$$

where δ symbolizes terms linear in V_0^{3J} for $J \neq 3$ and δ^2 symbolizes terms proportional to $V_0^{*3J} V_0^{3I}$ for $J, I \neq 3$, so that

$$(\mathbf{M}_d)_0^{JI} = m_{d_J} (1 + \epsilon_J \tan \beta) \quad (94)$$

$$(\delta \mathbf{M}_d)^{JI} = \begin{cases} m_{d_J} \epsilon_Y y_t^2 \tan \beta V_0^{3J*} & J \neq 3 = I \\ m_b \epsilon_Y y_t^2 \tan \beta V_0^{3I} & J = 3 \neq I \\ 0 & \text{otherwise} \end{cases} \quad (95)$$

$$(\delta^2 \mathbf{M}_d)^{JI} = \begin{cases} m_{d_J} \epsilon_Y y_t^2 \tan \beta V_0^{3J*} V_0^{3I} & (J, I) = (1, 2), (2, 1) \\ 0 & \text{otherwise} \end{cases}. \quad (96)$$

Now as we have second order terms explicitly in the mass matrix we need to expand the diagonalization matrices to second order. Additionally they have to be unitary to second order and the mass eigenvalues need to be real, which leads to the form

$$(\mathbf{D}_L)^{JI} = (\mathbf{1} + \delta \mathbf{D}_L + \delta^2 \mathbf{D}_L + \frac{1}{2} \delta \mathbf{D}_L \delta \mathbf{D}_L)^{JI} \quad (97)$$

$$(\mathbf{D}_L^\dagger)^{JI} = (\mathbf{1} - \delta \mathbf{D}_L - \delta^2 \mathbf{D}_L + \frac{1}{2} \delta \mathbf{D}_L \delta \mathbf{D}_L)^{JI} \quad (98)$$

$$(\mathbf{D}_R)^{JI} = (\mathbf{1} + \delta \mathbf{D}_R + \delta^2 \mathbf{D}_R + \frac{1}{2} \delta \mathbf{D}_R \delta \mathbf{D}_R)^{JI} e^{i\theta_I} \quad (99)$$

$$(\mathbf{D}_R^\dagger)^{JI} = (\mathbf{1} - \delta \mathbf{D}_R - \delta^2 \mathbf{D}_R + \frac{1}{2} \delta \mathbf{D}_R \delta \mathbf{D}_R)^{JI} e^{-i\theta_J}. \quad (100)$$

where $\delta\mathbf{D}_{\mathbf{L},\mathbf{R}}^\dagger = -\delta\mathbf{D}_{\mathbf{L},\mathbf{R}}$ and $\delta^2\mathbf{D}_{\mathbf{L},\mathbf{R}}^\dagger = -\delta^2\mathbf{D}_{\mathbf{L},\mathbf{R}}$. Now the requirement $\mathbf{D}_{\mathbf{L},\mathbf{R}}$ diagonalize the mass matrix $\mathbf{M}_{\mathbf{d}}$ for diagonal elements gives us the condition

$$\bar{m}_{d_J} \approx m_{d_J}|1 + \epsilon_J \tan \beta| \quad (101)$$

$$\theta_J \approx \arg(1 + \epsilon_J \tan \beta) \quad (102)$$

where we have only kept the leading order behaviour (i.e. δ^2 terms have been neglected).

All off-diagonal terms automatically vanish at the zeroth order and the first order contributions are the same as in Ref. [19]

$$e^{-i\theta_J}(-(\delta\mathbf{D}_{\mathbf{R}})(\mathbf{M}_{\mathbf{d}})_0 + \delta\mathbf{M}_{\mathbf{d}} + (\mathbf{M}_{\mathbf{d}})_0(\delta\mathbf{D}_{\mathbf{L}}))^{JI} = 0. \quad (103)$$

Which give us the results

$$(\delta\mathbf{D}_{\mathbf{L}})^{JI} = -\frac{(\mathbf{M}_{\mathbf{d}}^{\dagger JJ})_0(\delta\mathbf{M}_{\mathbf{d}})^{JI} + (\delta\mathbf{M}_{\mathbf{d}}^{\dagger})^{JI}(\mathbf{M}_{\mathbf{d}}^{II})_0}{|(\mathbf{M}_{\mathbf{d}}^{JJ})_0|^2 - |(\mathbf{M}_{\mathbf{d}}^{II})_0|^2} \quad (104)$$

$$(\delta\mathbf{D}_{\mathbf{R}})^{JI} = -\frac{(\mathbf{M}_{\mathbf{d}}^{JJ})_0(\delta\mathbf{M}_{\mathbf{d}}^{\dagger})^{JI} + (\delta\mathbf{M}_{\mathbf{d}})^{JI}(\mathbf{M}_{\mathbf{d}}^{\dagger II})_0}{|(\mathbf{M}_{\mathbf{d}}^{JJ})_0|^2 - |(\mathbf{M}_{\mathbf{d}}^{II})_0|^2}. \quad (105)$$

As $\delta\mathbf{M}_{\mathbf{d}} = 0$ for $(J, I) = (1, 2), (2, 1)$ these first order corrections are zero for these elements. To find the leading order contributions to $\mathbf{D}_{\mathbf{L},\mathbf{R}}$ for these components we need to go to quadratic order in the expansion parameter. Therefore the condition on the leading contributions to $\mathbf{D}_{\mathbf{L},\mathbf{R}}$ for $(J, I) = (1, 2), (2, 1)$ are

$$e^{-i\theta_J}(-(\delta^2\mathbf{D}_{\mathbf{R}})(\mathbf{M}_{\mathbf{d}})_0 + \Lambda + (\mathbf{M}_{\mathbf{d}})_0(\delta^2\mathbf{D}_{\mathbf{L}}))^{JI} = 0 \quad (106)$$

where

$$\begin{aligned} \Lambda^{JI} &= (\delta\mathbf{D}_{\mathbf{R}})^{\mathbf{J3}}((\delta\mathbf{M}_{\mathbf{d}})^{\mathbf{3I}} + (\delta\mathbf{D}_{\mathbf{L}})^{\mathbf{3I}}(\mathbf{M}_{\mathbf{d}})_0^{\mathbf{33}}) - \frac{1}{2}(\delta\mathbf{D}_{\mathbf{R}})^{\mathbf{J3}}(\delta\mathbf{D}_{\mathbf{R}})^{\mathbf{3I}} - \\ &(\delta^2\mathbf{M}_{\mathbf{d}})^{\mathbf{JI}} - (\delta\mathbf{M}_{\mathbf{d}})^{\mathbf{J3}}(\delta\mathbf{D}_{\mathbf{L}})^{\mathbf{3I}} - \frac{1}{2}(\delta\mathbf{D}_{\mathbf{L}})^{\mathbf{J3}}(\delta\mathbf{D}_{\mathbf{L}})^{\mathbf{3I}}(\mathbf{M}_{\mathbf{d}})_0^{\mathbf{33}} \end{aligned} \quad (107)$$

$$\begin{aligned} &= \frac{1}{2}(\delta\mathbf{D}_{\mathbf{R}})^{\mathbf{J3}}(\delta\mathbf{D}_{\mathbf{R}})^{\mathbf{3I}} - (\delta^2\mathbf{M}_{\mathbf{d}})^{\mathbf{JI}} - (\delta\mathbf{M}_{\mathbf{d}})^{\mathbf{J3}}(\delta\mathbf{D}_{\mathbf{L}})^{\mathbf{3I}} \\ &-\frac{1}{2}(\delta\mathbf{D}_{\mathbf{L}})^{\mathbf{J3}}(\delta\mathbf{D}_{\mathbf{L}})^{\mathbf{3I}}(\mathbf{M}_{\mathbf{d}})_0^{\mathbf{33}}. \end{aligned} \quad (108)$$

To arrive at Eq.(108) we used Eq.(103) and neglected terms of order $\mathcal{O}(m_{d_I}/m_b)$. Using Eq.(106) leads to a relation similar to the one in Eq.(104) and Eq.(105), except that $\delta\mathbf{M}_{\mathbf{d}} \rightarrow \Lambda$

$$(\delta^2\mathbf{D}_{\mathbf{L}})^{JI} = -\frac{(\mathbf{M}_{\mathbf{d}}^{\dagger JJ})_0(\Lambda)^{JI} + (\Lambda^{\dagger})^{JI}(\mathbf{M}_{\mathbf{d}}^{II})_0}{|(\mathbf{M}_{\mathbf{d}}^{JJ})_0|^2 - |(\mathbf{M}_{\mathbf{d}}^{II})_0|^2} \quad (109)$$

$$(\delta^2\mathbf{D}_{\mathbf{R}})^{JI} = -\frac{(\mathbf{M}_{\mathbf{d}}^{JJ})_0(\Lambda^{\dagger})^{JI} + \Lambda^{JI}(\mathbf{M}_{\mathbf{d}}^{\dagger II})_0}{|(\mathbf{M}_{\mathbf{d}}^{JJ})_0|^2 - |(\mathbf{M}_{\mathbf{d}}^{II})_0|^2}. \quad (110)$$

Substituting these equations into Eq. (104) and Eq.(105) and neglecting all terms suppressed by the mass hierarchy we find

$$(\delta \mathbf{D}_L)^{JI} = \begin{cases} -\frac{\epsilon_Y y_t^2 \tan \beta}{1+\epsilon_J \tan \beta} V_0^{3I} & J = 3 \neq I \\ \frac{\epsilon_Y^* y_t^2 \tan \beta}{1+\epsilon_J^* \tan \beta} V_0^{3J*} & J \neq 3 = I \\ 0 & \text{otherwise} \end{cases} \quad (111)$$

and

$$(\delta \mathbf{D}_R)^{JI} = \begin{cases} -\frac{\bar{m}_{dI}}{\bar{m}_b} \left(\frac{\epsilon_Y y_t^2 \tan \beta}{1+\epsilon_3 \tan \beta} + \frac{\epsilon_Y^* y_t^2 \tan \beta}{1+\epsilon_1^* \tan \beta} \right) e^{i(\theta_3-\theta_I)} V_0^{3I} & J = 3 \neq I \\ \frac{\bar{m}_{dJ}}{\bar{m}_b} \left(\frac{\epsilon_Y y_t^2 \tan \beta}{1+\epsilon_J \tan \beta} + \frac{\epsilon_Y^* y_t^2 \tan \beta}{1+\epsilon_3^* \tan \beta} \right) e^{i(\theta_J-\theta_3)} V_0^{3J*} & J \neq 3 = I \\ 0 & \text{otherwise} \end{cases} \quad (112)$$

Now to calculate the leading order corrections to the $(J, I) = (2, 1), (1, 2)$ elements we substitute the independent and linear order terms into Eq.(109) and Eq.(110) to find

$$(\delta^2 \mathbf{D}_L)^{21} = V_0^{32*} V_0^{31} \left(-\frac{\epsilon_Y y_t^2 \tan \beta}{1+\epsilon_2 \tan \beta} + \frac{\epsilon_Y^2 y_t^4 \tan^2 \beta}{(1+\epsilon_2 \tan \beta)(1+\epsilon_3 \tan \beta)} + \frac{|\epsilon_Y|^2 y_t^4 \tan^2 \beta}{2|1+\epsilon_3 \tan \beta|^2} \right) \quad (113)$$

$$(\delta^2 \mathbf{D}_R)^{21} = V_0^{32*} V_0^{31} \frac{\bar{m}_d}{\bar{m}_s} e^{i(\theta_2-\theta_1)} \left[-\left(\frac{\epsilon_Y y_t^2 \tan \beta}{1+\epsilon_2 \tan \beta} + \frac{\epsilon_Y^* y_t^2 \tan \beta}{1+\epsilon_1^* \tan \beta} \right) + \frac{|\epsilon_Y|^2 y_t^4 \tan^2 \beta}{|1+\epsilon_3 \tan \beta|^2} + \frac{(\epsilon_Y^*)^2 y_t^4 \tan^2 \beta}{(1+\epsilon_1^* \tan \beta)(1+\epsilon_3^* \tan \beta)} + \frac{\epsilon_Y^2 y_t^4 \tan^2 \beta}{(1+\epsilon_2 \tan \beta)(1+\epsilon_3 \tan \beta)} \right] \quad (114)$$

Using Eq.(111), Eq.(112), Eq.(113) and Eq.(114), we find the same corrections to the effective CKM matrix to leading order as in Refs. [19, 17, 15, 16]

$$V_0^{JI} = \begin{cases} V_{eff}^{3I} \frac{1+\epsilon_3 \tan \beta}{1+\epsilon_3^* \tan \beta} & J = 3 \neq I \\ V_{eff}^{J3} \frac{1+\epsilon_3^* \tan \beta}{1+\epsilon_3 \tan \beta} & J \neq 3 = I \\ V_{eff}^{JI} & \text{otherwise} \end{cases} \quad (115)$$

A.1.2 Flavor changing effective couplings of the Neutral Higgs Bosons

Using the relations derived in the previous section, it is relatively straightforward to calculate the coupling of the neutral Higgs bosons to the quarks. The effective lagrangian in the initial basis has the form

$$\mathcal{L}_{eff} = -(\bar{d}_J^0)_R \mathbf{F}_L^{\text{dS}} (d_I^0)_L S^0 - (\bar{d}_J^0)_L \mathbf{F}_R^{\text{dS}} (d_I^0)_R S^0 \quad (116)$$

where S^0 can be any of the three neutral scalars which has mixing matrix elements x_d^S for the Φ_d^{0*} Higgs and x_u^S for the Φ_u^{0*} Higgs. So if O^{IJ} diagonalizes the neutral Higgs mass matrix, we have

$$\begin{aligned} x_d^S &= O^{1S} + i \sin \beta O^{3S} \\ x_u^S &= O^{2S} - i \cos \beta O^{3S} \end{aligned} \quad (117)$$

Now if we rotate quarks into the physical basis the Lagrangian has the form

$$\mathcal{L}_{eff} = -(\bar{d}_J)_R \left(\mathbf{D}_R^\dagger \mathbf{F}_L^{\text{dS}} \mathbf{D}_L \right) (d_I)_L S^0 - (\bar{d}_J)_L \left(\mathbf{D}_L^\dagger \mathbf{F}_L^{\text{dS}} \mathbf{D}_R \right) (d_I^0)_R S^0 \quad (118)$$

Therefore, assuming a mass matrix of the form given in Eq. (92), we obtain,

$$(\mathbf{F}_L^{\text{dS}})^{JI} = \frac{m_{dJ}}{v_d} \left((x_d^S + \epsilon_J x_u^S) \delta^{JI} + \epsilon_Y y_t^2 x_u^S \lambda_0^{JI} \right). \quad (119)$$

which has a dependence up to second order on the CKM elements. Therefore, we obtain the following expansion in terms of CKM elements

$$\mathbf{F}_L^{\text{dS}} = (\mathbf{F}_L^{\text{dS}})_0 + \delta \mathbf{F}_L^{\text{dS}} + \delta^2 \mathbf{F}_L^{\text{dS}} \quad (120)$$

where

$$(\mathbf{F}_L^{\text{dS}})_0^{JI} = \frac{\bar{m}_{dJ} e^{i\theta_J}}{v_d (1 + \epsilon_J \tan \beta)} (x_d^S + \epsilon_J x_u^S) \delta^{JI} \quad (121)$$

$$(\delta \mathbf{F}_L^{\text{dS}})^{JI} = \begin{cases} \frac{\bar{m}_{dJ} e^{i\theta_J} \epsilon_Y y_t^2 x_u^S}{v_d (1 + \epsilon_J \tan \beta)} V_0^{3J*} & J \neq 3 = I \\ \frac{\bar{m}_{d3} e^{i\theta_3} \epsilon_Y y_t^2 x_u^S}{v_d (1 + \epsilon_3 \tan \beta)} V_0^{3I} & J = 3 \neq I \\ 0 & \text{otherwise} \end{cases} \quad (122)$$

$$(\delta^2 \mathbf{F}_L^{\text{dS}})^{JI} = \begin{cases} \frac{\bar{m}_{dJ} e^{i\theta_J} \epsilon_Y y_t^2 x_u^S}{v_d (1 + \epsilon_J \tan \beta)} V_0^{3J*} V_0^{3I*} & (J, I) = (1, 2), (2, 1) \\ 0 & \text{otherwise} \end{cases}. \quad (123)$$

Therefore the leading order contribution to the diagonal terms of ddS^0 coupling is just Eq. (121). Again the zeroth term makes no contribution to the off diagonal elements of the ddS couplings. Hence, at linear order we have for $J \neq I$

$$\begin{aligned} \delta \left(\mathbf{D}_R^\dagger \mathbf{F}_L^{\text{dS}} \mathbf{D}_L \right)^{JI} &= e^{-i\theta_J} \left(-(\delta \mathbf{D}_R)^{\text{JI}} (\mathbf{F}_L^{\text{dS}})_0^{\text{II}} + (\delta \mathbf{F}_L^{\text{dS}})^{\text{JI}} + \right. \\ &\quad \left. (\mathbf{F}_L^{\text{dS}})_0^{\text{JJ}} (\delta \mathbf{D}_L)^{\text{JI}} \right) \end{aligned} \quad (124)$$

which also disappears for $(J, I) = (1, 2), (2, 1)$. So the only contributions that are none zero at this order are when either $J = 3$ or $I = 3$. Using Eq. (111), Eq. (112), Eq. (115) and Eq. (122) and neglecting terms suppressed by the mass hierarchy we find that

$$\begin{aligned} (X_{RL}^S)^{JI} &= \delta \left(\mathbf{D}_R^\dagger \mathbf{F}_L^{\text{dS}} \mathbf{D}_L \right)^{JI} = \\ &\begin{cases} \frac{\bar{m}_b \epsilon_Y y_t^2}{v_d (1 + \epsilon_3 \tan \beta) (1 + \epsilon_0^3 \tan \beta)} V_{eff}^{3I} (x_u^S - x_d^S \tan \beta) & J = 3 \neq I \\ \frac{\bar{m}_{dJ} y_t^2 \Gamma^{J3}}{v_d (1 + \epsilon_3 \tan \beta) (1 + \epsilon_J \tan \beta)} V_{eff}^{3J*} (x_u^S - x_d^S \tan \beta) & J \neq 3 = I \\ 0 & \text{otherwise} \end{cases} \end{aligned} \quad (125)$$

where

$$\Gamma^{J3} = \frac{\epsilon_Y(1 + \epsilon_3^* \tan \beta) - \epsilon_Y^*(\epsilon_3 - \epsilon_J) \tan \beta}{1 + \epsilon_0^{3*} \tan \beta} \quad (126)$$

Finally to find the leading corrections to qqH coupling for $(J, I) = (2, 1), (1, 2)$ we need to go to quadratic order in which case we have

$$\begin{aligned} (X_{RL}^S)^{21} &= \delta^2 \left(\mathbf{D}_R^\dagger \mathbf{F}_L^{\text{dS}} \mathbf{D}_L \right)^{21}, \\ &= \frac{\bar{m}_s y_t^2 \Gamma^{21} (x_u^S - x_d^S \tan \beta)}{v_d (1 + \epsilon_2 \tan \beta) (1 + \epsilon_3 \tan \beta)} V_{eff}^{32*} V_{eff}^{31} \end{aligned} \quad (127)$$

$$\begin{aligned} (X_{RL}^S)^{12} &= \delta^2 \left(\mathbf{D}_R^\dagger \mathbf{F}_L^{\text{dS}} \mathbf{D}_L \right)^{12} \\ &= \frac{\bar{m}_d y_t^2 \Gamma^{12} (x_u^S - x_d^S \tan \beta)}{v_d (1 + \epsilon_1 \tan \beta) (1 + \epsilon_3 \tan \beta)} V_{eff}^{31*} V_{eff}^{32}, \end{aligned} \quad (128)$$

where

$$\begin{aligned} \Gamma^{21} &= \frac{\epsilon_Y}{(1 + \epsilon_2 \tan \beta) |1 + \epsilon_0^3 \tan \beta|^2} \left[(1 + \epsilon_0^3 \tan \beta) |1 + \epsilon_3 \tan \beta|^2 - \right. \\ &\quad \left. \epsilon_Y y_t^2 \tan \beta (1 + \epsilon_3^* \tan \beta) (1 + \epsilon_2 \tan \beta) - \right. \\ &\quad \left. \epsilon_Y^* y_t^2 \tan \beta (1 + \epsilon_2 \tan \beta)^2 \right], \end{aligned} \quad (129)$$

$$\begin{aligned} \Gamma^{12} &= \frac{\epsilon_Y}{(1 + \epsilon_2 \tan \beta) |1 + \epsilon_0^3 \tan \beta|^2} \left\{ (1 + \epsilon_0^3 \tan \beta) |1 + \epsilon_3 \tan \beta|^2 - \right. \\ &\quad \left. \epsilon_Y y_t^2 \tan \beta (1 + \epsilon_3^* \tan \beta) (1 + \epsilon_2 \tan \beta) - \epsilon_Y^* y_t^2 \tan \beta (1 + \epsilon_2 \tan \beta) \right. \\ &\quad \left. (1 + \epsilon_1 \tan \beta) + \frac{\epsilon_1 - \epsilon_2}{\epsilon_Y} \left[\frac{\epsilon_Y^* \tan \beta}{1 + \epsilon_2^* \tan \beta} \right. \right. \\ &\quad \left. \left. - \frac{(\epsilon_Y^*)^2 \tan^2 \beta y_t^2}{(1 + \epsilon_2^* \tan \beta) (1 + \epsilon_3^* \tan \beta)} - \frac{|\epsilon_Y|^2 \tan^2 \beta y_t^2}{|1 + \epsilon_3 \tan \beta|^2} \right] \right\}. \end{aligned} \quad (130)$$

In the limit that ϵ_0^J 's are uniform then of leading order contributions will collapse to Eq. (27) as each of Γ^{IJ} elements go to ϵ_Y . As the effective lagrangian is real, the LR couplings are related to RL , so that

$$X_{LR}^S = (X_{RL}^S)^\dagger. \quad (131)$$

A.2 Calculation of Loop factors

The assumption that the squark mass matrices are block diagonal in the tree level CKM basis gives us

$$\mathcal{M}_D^2 = \begin{pmatrix} (M_Q^2)_J \delta^{JI} & \frac{1}{\sqrt{2}} y_{d_j} \hat{\mu}_j^* v_u \delta^{JI} \\ \frac{1}{\sqrt{2}} y_{d_j} \hat{\mu}_j v_u \delta^{JI} & (M_D^2)_J \delta^{JI} \end{pmatrix} \quad (132)$$

$$\mathcal{M}_U^2 = \begin{pmatrix} (M_Q^2)_J \delta^{JI} + m_t^2 \delta^{J3} \delta^{I3} & -\frac{1}{\sqrt{2}} y_{u_j} \tilde{\mu}_j^* v_u \delta^{JI} \\ -\frac{1}{\sqrt{2}} y_{u_j} \tilde{\mu}_j v_u \delta^{JI} & (M_U^2)_J \delta^{JI} + m_t^2 \delta^{J3} \delta^{I3} \end{pmatrix} \quad (133)$$

where $\tilde{\mu}_J = \frac{\mu}{\tan\beta} - A_{u,J}$ and $\hat{\mu}_J = \mu - \frac{A_{d,J}}{\tan\beta}$. Therefore the diagonalization matrices have the simple form

$$Z_{(U,D)} = \begin{pmatrix} \delta^{IJ} \cos \alpha_I^{(U,D)} & \delta^{IJ} e^{-i\phi_I^{(U,D)}} \sin \alpha_I^{(U,D)} \\ -\delta^{IJ} e^{i\phi_I^{(U,D)}} \sin \alpha_I^{(U,D)} & \delta^{IJ} \cos \alpha_I^{(U,D)} \end{pmatrix} \quad (134)$$

where ϕ_I^D (ϕ_I^U) is the phase of $\hat{\mu}$ ($\tilde{\mu}$) and

$$\cot 2\alpha_J^D = -\frac{(m_Q^2)_J - (m_D^2)_J}{\sqrt{2}y_{d,J}|\hat{\mu}_J|v_u} \quad (135)$$

$$\cot 2\alpha_J^U = \frac{(m_Q^2)_J - (m_U^2)_J}{\sqrt{2}y_{u,J}|\tilde{\mu}_J|v_u} \quad (136)$$

Following the notation of Ref. [35] Z_+ and Z_- diagonalize the chargino mass matrix and Z_N and Z_N^T diagonalize the neutralino mass matrix. Additionally, if there is a splitting in the mass spectrum so that the squarks of the first two generation have uniform masses (i.e. $m_{D_1} = m_{D_2} = m_{D_4} = m_{D_5} = m_{U_1} = m_{U_2} = m_{U_4} = m_{U_5} = M_{SUSY}$) we find

$$\begin{aligned} \epsilon_0^J &= \frac{1}{16\pi^2 v_u} \left(\frac{32\pi\alpha_s}{3} M_3 \mu^* v_u C_0(|M_3|^2, m_{D_J}^2, m_{D_{J+3}}^2) + \right. \\ &\quad \left. \sum_{l=1}^4 m_{N_l} \left(P_D^{lJ} C_2(m_{N_l}^2, m_{D_J}^2, m_{D_{J+3}}^2) + Q_D^{lJ} C_0(m_{N_l}^2, m_{D_J}^2, m_{D_{J+3}}^2) \right) - \right. \\ &\quad \left. \sqrt{2} \sum_{l=1}^2 m_{C_l} Z_-^{1l} Z_+^{2l} \left(C_2(m_{C_l}^2, M_{SUSY}^2, M_{SUSY}^2) + M_{SUSY}^2 C_0(m_{N_l}^2, M_{SUSY}^2, M_{SUSY}^2) \right) \right) \end{aligned} \quad (137)$$

$$\begin{aligned} \epsilon_Y &= \frac{1}{16\pi^2 v_u} \sum_{l=1}^2 m_{C_l} \left[-\sqrt{2} \frac{g_2}{y_t^2} Z_-^{2l} Z_+^{1l} \left(C_2(m_{C_l}^2, m_{U_3}^2, m_{U_6}^2) + \right. \right. \\ &\quad \left. \left. (M_{U_3}^2 + m_t^2) C_0(m_{C_l}^2, m_{U_3}^2, m_{U_6}^2) - C_2(m_{C_l}^2, M_{SUSY}^2, M_{SUSY}^2) - \right. \right. \\ &\quad \left. \left. M_{SUSY}^2 C_0(m_{C_l}^2, M_{SUSY}^2, M_{SUSY}^2) \right) - Z_-^{2l} Z_+^{2l} \tilde{\mu}_3 v_u C_0(m_{C_l}^2, m_{U_3}^2, m_{U_6}^2) \right] \end{aligned} \quad (138)$$

where C_i are the Passarino-Veltman functions, m_i are the physical squark masses, M_i are the squark soft mass parameters and

$$P_D^{lJ} = Z_N^{3l} (g_1 Z_N^{1l} - g_2 Z_N^{2l}) \quad (139)$$

$$\begin{aligned} Q_D^{lJ} &= -\frac{g_1 Z_N^{1l}}{3} \hat{\mu}_J^* v_u \left(\frac{g_1 Z_N^{1l}}{3} - g_2 Z_N^{2l} \right) + \frac{2g_1 Z_N^{1l}}{3} Z_N^{3l} ((M_Q^2)_J + m_{d,J}^2) \\ &\quad + Z_N^{3l} \left(\frac{g_1 Z_N^{1l}}{3} - g_2 Z_N^{2l} \right) ((M_D^2)_J + (m_d^2)_J) - y_{d,J}^2 (Z_N^{3l})^2 \hat{\mu}_J v_u. \end{aligned} \quad (140)$$

Similarly for the antiholomorphic corrections to the up Yukawas have the form

$$\epsilon_0^{\prime J} = \frac{1}{16\pi^2 v_u} \left(-\frac{32\pi\alpha_s}{3} M_3 \mu^* v_u C_0(|M_3|^2, m_{U_J}^2, m_{U_{J+3}}^2) + \right.$$

$$\sum_{l=1}^4 m_{N_l} \left(P_U^{lJ} C_2(m_{N_l}^2, m_{U_J}^2, m_{U_{J+3}}^2) + Q_U^{lJ} C_0(m_{N_l}^2, m_{U_J}^2, m_{U_{J+3}}^2) \right) - \quad (141)$$

$$\sqrt{2} \sum_{l=1}^2 m_{C_l} Z_-^{1l} Z_+^{2l} \left(C_2(m_{C_l}^2, M_{SUSY}^2, M_{SUSY}^2) + M_{SUSY}^2 C_0(m_{N_l}^2, M_{SUSY}^2, M_{SUSY}^2) \right)$$

$$\epsilon'_Y = \frac{1}{16\pi^2 v_u} \sum_{l=1}^2 m_{C_l} \left[-\sqrt{2} \frac{g_2}{y_b^2} Z_+^{2l} Z_-^{1l} \left(C_2(m_{C_l}^2, m_{D_3}^2, m_{D_6}^2) + \right. \right.$$

$$\left. \left. (M_{D_3}^2 + m_b^2) C_0(m_{C_l}^2, m_{D_3}^2, m_{D_6}^2) - C_2(m_{C_l}^2, M_{SUSY}^2, M_{SUSY}^2) - \right. \right.$$

$$\left. \left. M_{SUSY}^2 C_0(m_{C_l}^2, M_{SUSY}^2, M_{SUSY}^2) \right) - Z_-^{2l} Z_+^{2l} \hat{\mu}_3 v_u C_0(m_{C_l}^2, m_{D_3}^2, m_{D_6}^2) \right] \quad (142)$$

where

$$P_U^{lJ} = -Z_N^{4l} (g_1 Z_N^{1l} - g_2 Z_N^{2l}) \quad (143)$$

$$Q_U^{lJ} = -\frac{2g_1 Z_N^{1l}}{3} \tilde{\mu}_J^* v_u \left(\frac{g_1 Z_N^{1l}}{3} + g_2 Z_N^{2l} \right) - \frac{4g_1 Z_N^{1l}}{3} Z_N^{4l} ((M_Q^2)_J + m_{u_J}^2)$$

$$+ Z_N^{4l} \left(\frac{g_1 Z_N^{1l}}{3} + g_2 Z_N^{2l} \right) ((M_U^2)_J + m_{d_J}^2) + y_{u_J}^2 (Z_N^{4l})^2 \tilde{\mu}_J v_u. \quad (144)$$

The infinities present in C_2 in ϵ_Y 's clearly cancel, however the infinities in ϵ_0 's need to be absorbed by counter terms in the effective lagrangian. So that the C_2 contributions to the ϵ 's in the above formulae are purely the finite pieces.

References

- [1] H. P. Nilles, Phys. Rept. **110** (1984) 1.
- [2] H. E. Haber and G. L. Kane, Phys. Rept. **117** (1985) 75.
- [3] M. Carena, J. Espinosa, M. Quirós and C. Wagner, *Phys. Lett.* **B 355** (1995) 209, hep-ph/9504316;
M. Carena, M. Quirós and C. Wagner, *Nucl. Phys.* **B 461** (1996) 407, hep-ph/9508343.
- [4] M. Carena, M. Quiros and C. E. M. Wagner, *Nucl. Phys. B* **461**, 407 (1996) [arXiv:hep-ph/9508343].
- [5] H.E. Haber, R. Hempfling and A.H. Hoang, *Z. Phys.* **C 75**, 539 (1997), [arXiv:hep-ph/9609331].
- [6] S. Heinemeyer, W. Hollik and G. Weiglein, *Eur. Phys. J. C* **9**, 343 (1999) [arXiv:hep-ph/9812472].
- [7] M. Carena, H. Haber, S. Heinemeyer, W. Hollik, C. Wagner, and G. Weiglein, *Nucl. Phys.* **B 580** (2000) 29, hep-ph/0001002.

- [8] J. Espinosa and R. Zhang, *Nucl. Phys. B* **586** (2000) 3, hep-ph/0003246.
- [9] A. Brignole, G. Degrassi, P. Slavich and F. Zwirner, *Nucl. Phys. B* **631** (2002) 195, hep-ph/0112177; *Nucl. Phys. B* **643** (2002) 79, hep-ph/0206101.
- [10] G. Degrassi, S. Heinemeyer, W. Hollik, P. Slavich and G. Weiglein, *Eur. Phys. J. C* **28** (2003) 133, hep-ph/0212020.
- [11] M. Carena and H. E. Haber, *Prog. Part. Nucl. Phys.* **50**, 63 (2003) [arXiv:hep-ph/0208209].
- [12] S. Heinemeyer, W. Hollik, H. Rzehak and G. Weiglein, *Eur. Phys. J. C* **39** (2005) 465, hep-ph/0411114.
- [13] S. Martin, *Phys. Rev. D* **67** (2003) 095012, hep-ph/0211366; *Phys. Rev. D* **71** (2005) 016012, hep-ph/0405022;
- [14] S. Bertolini, F. Borzumati, A. Masiero and G. Ridolfi, *Nucl. Phys. B* **353**, 591 (1991).
- [15] K. S. Babu and C. F. Kolda, *Phys. Rev. Lett.* **84**, 228 (2000) [arXiv:hep-ph/9909476].
- [16] C. Hamzaoui, M. Pospelov and M. Toharia, *Phys. Rev. D* **59**, 095005 (1999) [arXiv:hep-ph/9807350].
- [17] G. Isidori and A. Retico, *JHEP* **0111**, 001 (2001) [arXiv:hep-ph/0110121].
- [18] A. J. Buras, P. H. Chankowski, J. Rosiek and L. Slawianowska, *Phys. Lett. B* **546**, 96 (2002) [arXiv:hep-ph/0207241].
- [19] A. J. Buras, P. H. Chankowski, J. Rosiek and L. Slawianowska, *Nucl. Phys. B* **659**, 3 (2003) [arXiv:hep-ph/0210145].
- [20] A. Dedes and A. Pilaftsis, *Phys. Rev. D* **67**, 015012 (2003) [arXiv:hep-ph/0209306].
- [21] G. D'Ambrosio, G. F. Giudice, G. Isidori and A. Strumia, *Nucl. Phys. B* **645**, 155 (2002) [arXiv:hep-ph/0207036].
- [22] M. Dugan, B. Grinstein and L. J. Hall, *Nucl. Phys. B* **255**, 413 (1985).
- [23] J. Foster, K. i. Okumura and L. Roszkowski, *JHEP* **0508**, 094 (2005) [arXiv:hep-ph/0506146].
- [24] M. Carena, M. Quiros and C. E. M. Wagner, *Phys. Lett. B* **380**, 81 (1996) [arXiv:hep-ph/9603420]; *Nucl. Phys. B* **524**, 3 (1998) [arXiv:hep-ph/9710401].
- [25] B. de Carlos and J. R. Espinosa, *Nucl. Phys. B* **503**, 24 (1997) [arXiv:hep-ph/9703212].
- [26] M. Losada, *Nucl. Phys. B* **537**, 3 (1999) [arXiv:hep-ph/9806519].

- [27] M. Laine and K. Rummukainen, Nucl. Phys. B **535**, 423 (1998) [arXiv:hep-lat/9804019].
- [28] C. Balazs, M. Carena and C. E. M. Wagner, Phys. Rev. D **70**, 015007 (2004) [arXiv:hep-ph/0403224].
- [29] C. Balazs, M. Carena, A. Menon, D. E. Morrissey and C. E. M. Wagner, Phys. Rev. D **71**, 075002 (2005) [arXiv:hep-ph/0412264].
- [30] H. Eberl, K. Hidaka, S. Kraml, W. Majerotto and Y. Yamada, *Phys. Rev. D* **62** (2000) 055006, hep-ph/9912463.
- [31] M. Carena, D. Garcia, U. Nierste and C. Wagner, *Nucl. Phys. B* **577** (2000) 577, hep-ph/9912516.
- [32] R. Hempfling, *Phys. Rev. D* **49** (1994) 6168;
L. Hall, R. Rattazzi and U. Sarid, *Phys. Rev. D* **50** (1994) 7048, hep-ph/9306309;
M. Carena, M. Olechowski, S. Pokorski and C. Wagner, *Nucl. Phys. B* **426** (1994) 269, hep-ph/9402253.
- [33] A. Pilaftsis and C. E. M. Wagner, Nucl. Phys. B **553**, 3 (1999) [arXiv:hep-ph/9902371].
- [34] M. Carena, J. R. Ellis, S. Mrenna, A. Pilaftsis and C. E. M. Wagner, Nucl. Phys. B **659**, 145 (2003) [arXiv:hep-ph/0211467].
- [35] J. Rosiek, arXiv:hep-ph/9511250.
- [36] A. J. Buras, F. Parodi and A. Stocchi, JHEP **0301**, 029 (2003) [arXiv:hep-ph/0207101].
- [37] M. Battaglia *et al.*, arXiv:hep-ph/0304132.
- [38] UTFit Working Group, <http://www.utfit.org>
- [39] J. Charles *et al.* [CKMfitter Group], Eur. Phys. J. C **41**, 1 (2005) [arXiv:hep-ph/0406184];
http://www.slac.stanford.edu/xorg/ckmfitter/plots_eps2005/ckmEval_results_eps_05.ps
- [40] V. Abazov [D0 Collaboration], arXiv:hep-ex/0603029.
- [41] See the CDF webpage:
<http://www-cdf.fnal.gov/physics/new/bottom/060406.blessed-Bsmix/>
or I. Furic's talk at:
http://vmsstreamer1.fnal.gov/VMS_Site_03/Lectures/CDF/060410Furic/
- [42] R. Bernhard *et al.* [CDF Collaboration], arXiv:hep-ex/0508058.
- [43] <http://www-cdf.fnal.gov/physics/new/bottom/bottom.html>

- [44] C. Kounnas, A. B. Lahanas, D. V. Nanopoulos and M. Quiros, Nucl. Phys. B **236**, 438 (1984).
- [45] J. A. Casas, A. Lleyda and C. Munoz, Nucl. Phys. B **471**, 3 (1996) [arXiv:hep-ph/9507294].
- [46] S. Herrlich and U. Nierste, Phys. Rev. D **52**, 6505 (1995) [arXiv:hep-ph/9507262].
- [47] M. Carena, S. Heinemeyer, C. E. M. Wagner and G. Weiglein, Eur. Phys. J. C **26** (2003) 601 [arXiv:hep-ph/0202167].
- [48] R. Barbieri and G. F. Giudice, Phys. Lett. B **309**, 86 (1993) [arXiv:hep-ph/9303270].
- [49] M. Ciuchini, G. Degrassi, P. Gambino and G. F. Giudice, Nucl. Phys. B **527**, 21 (1998) [arXiv:hep-ph/9710335].
- [50] G. Degrassi, P. Gambino and G. F. Giudice, JHEP **0012**, 009 (2000) [arXiv:hep-ph/0009337].
- [51] M. Carena, D. Garcia, U. Nierste and C. E. M. Wagner, Phys. Lett. B **499**, 141 (2001) [arXiv:hep-ph/0010003].
- [52] P. Gambino and M. Misiak, Nucl. Phys. B **611**, 338 (2001) [arXiv:hep-ph/0104034].
- [53] F. Borzumati, C. Greub and Y. Yamada, Phys. Rev. D **69**, 055005 (2004) [arXiv:hep-ph/0311151].
- [54] M. Neubert, Eur. Phys. J. C **40**, 165 (2005) [arXiv:hep-ph/0408179].
- [55] M. Carena, S. Heinemeyer, C. E. M. Wagner and G. Weiglein, arXiv:hep-ph/0511023.
- [56] http://www-cdf.fnal.gov/physics/exotic/r2a/20050519.mssm_htt/index.htm
- [57] T. Ibrahim and P. Nath, Phys. Rev. D **67**, 016005 (2003) [arXiv:hep-ph/0208142].
- [58] G. L. Kane, C. Kolda and J. E. Lennon, arXiv:hep-ph/0310042.
- [59] A. Dedes and B. T. Huffman, Phys. Lett. B **600**, 261 (2004) [arXiv:hep-ph/0407285].
- [60] Nikolai Nikitine, talk given at "FLAVOUR IN THE ERA OF THE LHC" Opening plenary meeting: CERN, November 7-10 2005;
R. McPherson, talk given at the Aspen Winter Conference, Aspen, CO, February 12-18, 2006, <http://www.aspenphys.org>
- [61] See, for example, B. Heinemann presentation to the P5 Committee, Fermilab, September 2006, <http://hep.ph.liv.ac.uk/~beate/homepage/p5-discovery.pdf>
- [62] S. Abdullin *et al.*, Eur. Phys. J. C **39S2**, 41 (2005).

- [63] S. Bertolini, F. Borzumati and A. Masiero, Phys. Lett. B **194**, 545 (1987) [Erratum-
ibid. B **198**, 590 (1987)].
- [64] R. Demina, J. D. Lykken, K. T. Matchev and A. Nomerotski, Phys. Rev. D **62**, 035011
(2000) [arXiv:hep-ph/9910275]
- [65] M. Carena, D. Choudhury, S. Raychaudhuri and C. E. M. Wagner, Phys. Lett. B **414**,
92 (1997) [arXiv:hep-ph/9707458].

